

Discovering Patterns in Multi-neuronal Spike Trains using the Frequent Episode Method

K.P.Unnikrishnan*and Debprakash Patnaik[†]and P.S.Sastry[‡]

ABSTRACT

Discovering the 'Neural Code' from multi-neuronal spike trains is an important task in neuroscience. For such an analysis, it is important to unearth interesting regularities in the spiking patterns. In this report, we present an efficient method for automatically discovering synchrony, synfire chains, and more general sequences of neuronal firings. We use the Frequent Episode Discovery framework of Laxman, Sastry, and Unnikrishnan (2005), in which the episodes are represented and recognized using finite-state automata. Many aspects of functional connectivity between neuronal populations can be inferred from the episodes. We demonstrate these using simulated multi-neuronal data from a Poisson model. We also present a method to assess the statistical significance of the discovered episodes. Since the Temporal Data Mining (TDM) methods used in this report can analyze data from hundreds and potentially thousands of neurons, we argue that this framework is appropriate for discovering the 'Neural Code'.

1 INTRODUCTION

Analyzing spike trains from hundreds of neurons is an important and exciting problem. By using experimental techniques such as Micro Electrode Arrays or imaging of neural currents through voltage-sensitive dyes etc., spike data can be recorded simultaneously from many neurons [1, 2]. Automatically discovering

*General Motors R&D Center, Warren, MI

[†]Dept. Electrical Engineering, Indian Institute of Science, Bangalore

[‡]Dept. Electrical Engineering, Indian Institute of Science, Bangalore

patterns (regularities) in these spike trains can lead to better understanding of the functional relationships within the system that produced the spikes. Such understanding of functional relations embedded in spike trains lead to many applications, e.g., better brain-machine interfaces. Such an analysis can also ultimately allow us to systematically answer the question, "is there a neural code?".

In this paper, we present some novel methods to analyze spike train data, based on the method of frequent episode discovery in time-ordered event sequences [3, 4, 5], which is from the field of temporal data mining. Temporal data mining is concerned with analysis of large sequential data sets [6]. Such data sets with temporal dependencies frequently occur in many business, engineering and scientific scenarios. Frequent episode discovery, originally proposed in [3], is one of the popular frameworks in temporal data mining. Here, the data is viewed as a time-ordered sequence of events where each event is characterized by an event type and a time of occurrence. A few examples of such data are alarms in a telecommunication network, fault logs of a manufacturing plant etc. The goal of the analysis is to unearth temporal patterns (called episodes) that occur sufficiently often along that sequence. These discovered patterns are called frequent episodes. The multi-neuronal spike train data is also a sequential or time-ordered data stream of events where each event is a spike at a particular time and the event type would be the neuron (or the electrode in the micro electrode array) that generated the spike. Since functionally interconnected neurons tend to fire in certain precise patterns, discovering frequent patterns in such temporal data can help understand the underlying neural circuitry. In this paper, we argue that the frequent episodes framework is ideally suited for such analysis. There are efficient algorithms for automatically detecting many types of frequent episodes [3, 4]. However, as we shall see, in analyzing neural spiking data, one needs methods that can discover frequent episodes under different kinds of temporal constraints. We explain some datamining algorithms for frequent episode discovery under such temporal constraints [5]. Through extensive simulation studies using both synthetic and real neural data, we argue that the frequent episodes framework is ideally suited for this application. We show that these datamining techniques provide a very efficient and general purpose methodology for detecting many types of interesting patterns in spike

data.

Most of the currently available methods for analyzing spike train data rely on quantities that can be computed through cross correlations among spike trains (time shifted with respect to one another) to identify interesting patterns in spiking activity. There are methods to look for specific patterns and assess their statistical significance under a null hypothesis that different spike trains are *iid* Bernoulli processes [7, 8, 9]. Most such methods can not look for patterns that involve more than 3 or 4 neurons due to the ubiquitous curse of dimensionality. Looking for repeated occurrences of patterns of firing involving many neurons becomes infeasible due to the combinatorial explosion of candidate patterns that one should look for. The data mining approach tackles this by adopting the same basic idea as in the Apriori algorithm [10], first proposed in the context of discovering association rules involving many items in a large data base. This idea has been extended to sequential data streams and the frequent episode discovery methods that we propose here are based on the same idea.

We show here that, by adopting such a data mining method, we can efficiently *discover* important regularities in the multi-neuronal spike sequences. We illustrate this using simulated as well as real spike sequences. We use a simulator where each neuron is modelled as an inhomogeneous Poisson process whose firing rate is modified based on the input received from other neurons. We also implement the refractory period by filtering out spikes (generated under the Poisson process) that are too close to the previous spike, before they reach any down-stream neuron. Using this simulator, we also show that we can assess statistical significance of the detected patterns. (This is done using the same idea as in the ‘jitter’ method [11]). In addition to the results on simulated spike trains, we also show the effectiveness of our approach by analyzing some data obtained through micro-electrode array experiments.

Rest of the paper is organized as follows. Section 2 presents a brief review of analysis of multi-neuronal spike trains. In Section 3 we briefly explain our method of frequent episode discovery and discuss how this method can be used to infer interesting patterns in spike train data. The algorithms for discovering frequent episodes under different temporal constraints are explained in the next two sections. We explain our simulation model and present the results obtained in Section 5. The paper is concluded with a discussion of the method and the

many possibilities it offers, in Section 6.

2 Multi-neuronal Data Analysis

Over the last couple of decades, increasingly better methods are becoming available for simultaneously recording the activities of hundreds of neurons [7, 12, 13, 14, 15, 16, 1, 17, 2] and hence development of efficient algorithms to analyze multi-neuronal spike trains is becoming critical. This field has a long history, beginning with the work of Gerstien and his colleagues [18] and a recent review [19] summarizes three decades of development in this area.

Microelectrode array (MEA) is a popular technology for simultaneously recording the spike signals from many neurons and has now become a standard method used in experiments with neuronal ensembles. A typical MEA setup consists of 8×8 grid of 64 electrodes with inter-electrode spacing of about 25 microns and can be mounted on a neural culture or brain slice. Other technologies for recording from multiple neurons include imaging of neuronal currents using some specialized dyes. One popular method here is to image the Calcium currents. These technologies now allow for gathering of vast amounts of data, especially in neuronal cultures, using which one wishes to study connectivity patterns and microcircuits in neural systems [2, 1].

The availability of vast amounts such data means that developing efficient methods to analyze neuronal spike trains is a challenging task of immediate utility in this area [19]. A major goal of such neural data analysis is to characterize how neurons that are part of an ensemble interact with each other.

The patterns that one is interested in can be roughly grouped into what are called Synchrony, Order and Synfire chains. Synchronous firing by a group of neurons is interesting because it can be an efficient way to transmit information [20]. One can identify synchronous firing of neurons by analyzing cross correlation of spike trains [21, 22, 23]. Ordered firing sequences of neurons where times between firing of successive neurons are fairly constant denote a chain of triggering events and unearthing such relations between neurons can thus reveal some microcircuits [24]. Discovering temporally ordered firing sequences is important for understanding functional connectivity. If neuron A is functionally connected to neuron B, it influences the firing of neuron B. If this is an excitatory connection (with or without a delay), then, if A fires, B is likely to fire soon after that.

Hence, discovering the order of neuronal firings can help decipher the functional connectivity. Memory traces are probably embedded in such sequential activations of neurons or neuronal groups. Signals of this form have recently been found in groups of hippocampal neurons by Lee and Wilson [25]. They used specialized algorithms to search for such ordered firings by a group of neurons (when these orders are known or suspected) [8]. There are also other algorithms for detecting ordered firing sequences with precise timing relationships [7, 9]. These methods are based on analyzing cross correlation of spike trains where one spike train is delayed with respect to the other. An ordered chain of firings of neuronal groups (rather than single neurons) is sometimes called a Synfire chain and is believed to be an important microcircuit [1]. A synfire chain can be thought of as a compound pattern involving both synchrony and order.

Discovering such interesting patterns in spike trains amounts to unearthing groups of neurons that fire in some kind of coordinated fashion. As already mentioned, in most of the currently available methods, the curse of dimensionality forces the analysis to be confined to a few variables at a time. For the same reason, it is often very difficult to *discover* all patterns of a particular kind. Thus, many of the available algorithms are for counting occurrences of specific list of patterns. In the next section we explain the idea of frequent episodes and show that this data mining viewpoint gives us a unified algorithmic scheme for discovering many types of interesting patterns in spike train data.

3 Frequent Episode Discovery

Frequent episode discovery framework was proposed by Mannila et.al. [3] in the context analyzing alarm sequences in a communication network. Laxman et.al. [4] introduced the notion of non-overlapped occurrences as episode frequency and proposed efficient counting algorithms. We first give brief overview of this framework.

In the frequent episodes framework, the data to be analyzed is a sequence of events denoted by $((E_1, t_1), (E_2, t_2), \dots)$ where E_i represents an *event type* and t_i the *time of occurrence* of the i^{th} event. E_i 's are drawn from a finite set of event types. The sequence is ordered with respect to time of occurrences of the events so that, $t_i \leq t_{i+1}$, for all $i = 1, 2, \dots$. The following is an example event

sequence containing 7 events with 5 event types.

$$\langle (A, 1), (B, 3), (D, 4), (C, 6), (A, 12), (E, 14), (B, 15) \rangle \quad (1)$$

In multi-neuron data, a spike event has the label of the neuron (or the electrode number in case of multi-electrode array recordings) which generated the spike as its event type and has the associated time of occurrence. The neurons in the ensemble under observation fire action potentials at different times, that is, generate spike events. All these spike events are strung together, in time order, to give a single long data sequence as needed for frequent episode discovery.

The general temporal patterns that we wish to discover in this framework are called episodes. In this paper we shall deal with two types of episodes: *Serial* and *Parallel*.

Formally, an episode α is a triple $(V_\alpha, \leq_\alpha, g_\alpha)$, where V_α is a set of nodes, \leq_α is a partial order on V_α , and $g_\alpha : V_\alpha \rightarrow \zeta$ (the set of event types), is a mapping associating each node with an event type. For an episode to occur in a data stream, the events in $g_\alpha(V_\alpha)$ have to occur in the order described by \leq_α . The size of α , denoted as $|\alpha|$, is $|V_\alpha|$ (i.e. the number of nodes in V_α). Episode α is a parallel episode if the partial order \leq_α is a null set. It is a serial episode if the relation \leq_α is a total order. A partial order which is neither a total order nor a null set corresponds to the most general class of episodes. Such episodes can be described by directed acyclic graphs.

A *serial episode* is an ordered tuple of event types. For example, $(A \rightarrow B \rightarrow C)$ is a 3-node serial episode. The arrows in this notation indicate the order of the event types. Such an episode is said to *occur* in an event sequence if there are corresponding events in the prescribed order. In sequence (1), the events $(A, 1), (B, 3), (C, 6)$ constitute an occurrence of the above episode. In contrast a *parallel episode* is similar to an unordered set of items. It does not require any specific ordering of the events. We denote a 3-node parallel episode with event types A, B and C , as (ABC) . An occurrence of (ABC) can have the events in any order in the sequence.

We note here that occurrence of an episode (of either type) does not require the associated event types to occur consecutively; there can be other intervening events between them. In the multi-neuronal data, if neuron A makes neuron B to fire, then, we expect to see B following A often. However, in different

occurrences of such a substring, there may be different number of other spikes between A and B because many other neurons may also be spiking simultaneously. Thus, the episode structure allows us to unearth patterns in the presence of such noise in spike data.

Subepisode: An episode β is a sub-episode of episode α if all event types of β are in α and if partial order among the event types of β is same as that for the corresponding event types in α . For example $(A \rightarrow B)$, $(A \rightarrow C)$, and $(B \rightarrow C)$ are 2-node sub-episodes of the 3-node episode $(A \rightarrow B \rightarrow C)$, while $(B \rightarrow A)$ is not. In case of parallel episodes, there is no ordering requirement. Hence every subset of the set of event types of an episode is a subepisode. It is to be noted here that occurrence of an episode implies occurrence of all its subepisodes.

Frequency of episodes: A frequent episode is one whose frequency exceeds a user specified threshold. The frequency of an episode can be defined in many ways. It is intended to capture some measure of how often an episode occurs in an event sequence. One chooses a measure of frequency so that frequent episode discovery is computationally efficient and, at the same time, higher frequency would imply that an episode is occurring often. For the results presented in this paper, we use the non-overlapped occurrences count as the frequency [4, 26].

Two occurrences of an episode are said to be *non-overlapped* if no event associated with one appears in between the events associated with the other. A collection of occurrences of α is said to be non-overlapped if every pair of occurrence in it is non-overlapped. The corresponding frequency for episode α is defined as the cardinality of the largest set of non-overlapped occurrences of α in the given event sequence. (See [4] for more discussion).

This definition of frequency results in very efficient counting algorithms [4]. It is also more intuitively satisfying because it counts a well defined subset of the set of all occurrences of an episode. In the context of our application, counting non-overlapped occurrences is natural because we would then be looking at causative chains that happen at different times again and again.

3.1 Temporal Constraints

As stated earlier, while analyzing neuronal spike data, it is useful to consider methods, where, while counting the frequency, we include only those occurrences which satisfy some additional temporal constraints. We mainly consider two

types of such constraints: episode expiry time and inter-event time constraints.

Given an episode occurrence (that is, a set of events in the data stream that constitute an occurrence of the episode), we call the largest time difference between any two events constituting the occurrence as the span of the occurrence. For serial episodes, this would be the difference between times of the first and last events of the episode (in an occurrence). The episode expiry time constraint requires that we count only those occurrences whose span is less than a (user-specified) time T_X . (In the algorithm in [3], the window width essentially implements an upper bound on the span of occurrences.) An efficient algorithm for counting non-overlapping occurrences of serial episodes that satisfy an expiry time constraint is available in [26]. However, currently there is no algorithm for counting occurrences parallel episodes under expiry time constraint. We present such an algorithm in the next section.

The inter-event time constraint, which is meaningful only for serial episodes, is specified by giving an interval of the form $(T_{low}, T_{high}]$ and requires that the difference between the times of every pair of successive events in any occurrence of a serial episode should be in this interval. In a generalized form of this constraint, we may have different time intervals for different pairs of events. In the next section, we present algorithms for counting non-overlapped occurrences of episodes with such inter-event time constraints. Our algorithm also discovers the most suitable interval constraint (choosing from a set of intervals) for each consecutive pair of events in the discovered frequent episodes. This leads to discovery of episodes under generalized inter-event time constraints.

In the next subsection we explain the importance of these temporal constraints for capturing many of the desired patterns in spike data in terms of frequent episodes. While these temporal constraints are motivated by our application, these are fairly general and would be useful in many other applications of frequent episode discovery.

3.2 Episodes as patterns in neuronal spike data

The analysis requirements of spike train data are met very well by the frequent episodes framework. Serial and parallel episodes with appropriate temporal constraints can capture many patterns of interest in multi-neuronal data. Fig. 1 shows some possibilities of neuronal interconnections that may give rise to dif-

ferent patterns in spike data.

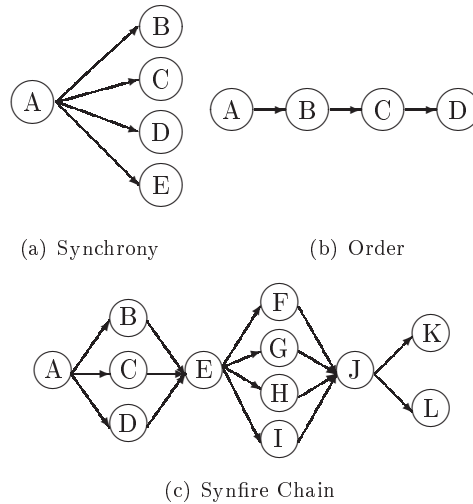


Figure 1: Examples of neuronal connection structures that can result in different patterns in the spike trains : (a). simple circuit that can generate synchronous firing patterns. Neurons B,C,D,E may fire synchronously, (b). simple circuit that generates firing of A, B, C, D in order, (c). A synfire chain pattern where different groups of synchronously firing neurons obey a serial order.

As stated earlier, one of the patterns of interest is Synchrony or co-spiking activity in which groups of neurons fire synchronously. This kind of synchrony may not be precise. That is, all neurons in the group need not fire at exactly the same instant of time. Allowing for some amount of variability, co-spiking activity requires that all neurons must fire within a small interval of time of each other (in any order) for them to be grouped together. Such synchronous firing patterns may be generated using the structure as shown in fig. 1(a). Such patterns of Synchrony can be discovered by looking for frequent parallel episodes which satisfy an expiry time constraint. For example, we can choose the expiry time to be less than a typical synaptic delay. The expiry time here controls the amount of variability allowed for declaring a grouped activity as synchronous.

Another pattern in spike data is ordered firings. A simple mechanism that can generate ordered firing sequences is shown in fig. 1(b). Serial episodes capture such a pattern very well. Once again, we may need some additional time constraints. A useful constraint is that of inter-event time constraint. In multi-neuron data, if we want to conclude that A is causing B to fire, then B

can not occur too soon after A because there would be some propagation delay and B can not occur too much later than A because the effect of firing of A would not last indefinitely. For example, we can prescribe that inter-event times should be in the range of one to two synaptic delay times so that a frequent serial episode may capture an underlying microcircuit. Thus, serial episodes with proper inter-event time constraints can capture ordered firing sequences which may be due to underlying functional connectivity.

Another important pattern in spiking data is that of synfire chains [1]. This consists of groups of synchronously firing neurons strung together with tight temporal constraints, repeating often. We can discover such synfire chains by combining parallel and serial episode discovery.

The structure shown in Fig. 1(c) captures such a synfire chain. We can think of this as a microcircuit where A primes synchronous firing of (BCD) , which, through E , causes synchronous firing of $(FGHI)$ and so on. When such a pattern occurs often in the spike train data, parallel episodes like (BCD) and $(FGHI)$ become frequent (by using appropriate expiry time constraint). After discovering all such parallel episodes, we replace all recognized occurrences of each of these episodes by a new event in the data stream with a new symbol (representing the episode) for the event type and an appropriate time of occurrence. Then we discover serial episodes on this new data stream. With this procedure, we can unearth patterns such as synfire chains.

Summarizing the above discussion, we can assert that frequent episode discovery with various temporal constraints gives us a lot of flexibility in the kind patterns that we can discover in multi-neuronal spiking data.

3.3 Algorithms for frequent episode discovery

As said earlier, there are efficient frequent episode discovery algorithms that can handle the required temporal constraints. There are also algorithms that can discover ‘useful’ inter-event time constraints automatically from the data. In this subsection, we briefly explain the basic idea in these algorithms. We give details of the algorithms needed for discovering parallel episodes with expiry time constraint and for discovering serial episodes with inter-event time constraints in the next section. The reader is referred to [4, 5] for more details regarding different algorithms for frequent episode discovery.

Consider the problem of discovering all frequent serial episodes upto a given size, say, n . The discovery process has two main steps. First, we build a set of candidate episodes and next we obtain the frequencies (i.e., count the non-overlapping occurrences) of the candidates in the data so that we can retain only those whose frequencies are above the user-set threshold.

Even if we assume only 50 neurons (or, in the jargon of datamining, event types), the number of possible n -node serial episodes would be unmanageably large even for n as small as 5. As stated earlier, it is this combinatorial explosion that limits all the current spike-data analysis techniques from being able to discover large sequential patterns. In the datamining methods, this is handled by using the idea of discovering progressively larger episodes, as we explain below.

Recall that, given a serial episode, any subsequence which conforms to the order of event types in the episode is called a subepisode. For now, let us assume that there are no temporal constraints. The key observation is that the episode can be frequent only if all its subepisodes are frequent. This is immediately obvious because, for example, given two non-overlapping occurrences of $A \rightarrow B \rightarrow C$, we have atleast two non-overlapping occurrences of each of its subepisodes. This immediately gives rise to a level-wise procedure for discovering all frequent episodes. First we discover all frequent 1-node episodes. (This is simply a histogram of event types). Then we build a set of candidate 2-node episodes such that the 1-node subepisodes of all candidates are seen to be frequent. Now through one more pass over the data, we count the non-overlapping occurrences of all the candidates and thus come out with frequent 2-node episodes. Now we combine only the frequent 2-node episodes to build a candidate set of 3-node episodes and so on. Thus at stage n , using the already discovered set of frequent n -node episodes, we build the set of candidate $(n + 1)$ -node episodes and by counting their occurrences in the data (using one more pass over the data), we come out with frequent $(n + 1)$ -node episodes. This procedure controls the combinatorial explosion because we are, after all, interested only in episodes that occur sufficiently often. By choosing a suitably large frequency threshold, as the size of episodes grows, the number of frequent episodes would come down. (It is highly unlikely that all large random sequences occur often in the data). Because of this, the number of candidates

becomes much much less than the combinatorially possible number, as the size of episodes grows.

Now let us examine whether this idea works even when we impose additional temporal constraints. Suppose we use expiry time constraint. Then each occurrence of an episode which completes within the expiry time also contains an occurrence of its subepisodes each of which also complete within the expiry time. Hence, once again all subepisodes would be at least as frequent as the episode. Next let us consider the inter-event time constraint. Now, it is no longer true that subepisodes are as frequent as episodes. This is because we may have many occurrences of $A \rightarrow B \rightarrow C$ where each pair of consecutive events occur within time, say, T_x , but there may be no occurrence of the episode $A \rightarrow C$ such that the time between the two events is less than T_x . So, it may appear that our nice level-wise procedure breaks down under inter-event time constraints. However, we observe that if we confine ourselves only to prefix and suffix subepisodes then, once again, frequency of subepisodes would be atleast as much as that of the episode. All we need is a slight change in the candidate generation strategy [5].

In a wide variety of data mining applications this strategy is seen to be very effective in controlling the combinatorial explosion. This basic idea is from the so called Apriori algorithm [10] in the context of discovering frequent itemsets. This is extended to the case of discovering episodes by Mannila [3]. The idea of non-overlapped occurrences as frequency makes the process of obtaining frequencies of episodes very fast. This and the extensions to tackle various temporal constraints are described in [4, 26, 5].

Given that we can control the growth of candidates as the size of episodes increases, the next question is how do we count the frequencies of a set of candidate episodes. This is done by having a finite state automaton for each episode such that it recognizes the occurrence of an episode. As we traverse the data, for each event (spike) we encounter, we make appropriate state changes in all the automata and whenever an automaton transits to its end state we increment the count of the corresponding episode. Thus, we can simultaneously count the occurrences of a set of candidates using a single pass over the data. The number of active automata per episode that we need (which is same as the temporary memory needed by the algorithm) depends on what all types of

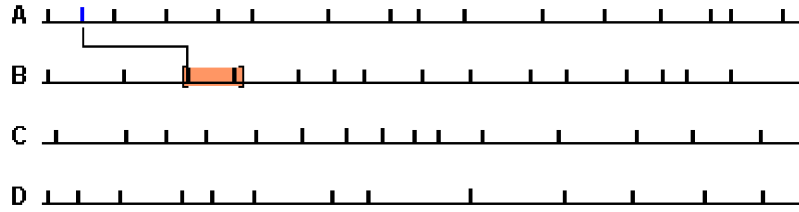
occurrences we want to count. Restricting the count to only non-overlapped occurrences makes the counting process also very efficient [4]. Later, we give full details of the candidate generation strategy and the counting procedure for two algorithms. Before that, we explain the basic idea of this counting (under inter-event time constraints) in Fig. 2

The first panel in the figure shows the spike data as a raster plot. For illustration, consider counting occurrences of the $A \rightarrow B \rightarrow C \rightarrow D$. At the beginning, there would be an automaton of this episode that is waiting for event type A . When we see an A , we make a state transition and then the automaton is waiting to see a B . This is shown in panel (b) in the figure. Now, due to the inter-event time constraint, this automaton needs a B within some window on the time axis as shown in panel (b). When we reach those time points, a B there can now cause a state transition in this automaton and it now starts waiting for C . However, there may be more than one B in the appropriate time window and we have to remember all these because, at this stage, we can not know which of these, if any, leads to an occurrence of the episode that satisfies the inter-event time constraints. (This is the reason we may need more than one active automaton per episode during the counting process). Logically this means that the automaton spawns multiple copies of itself. However, we can design efficient data structures to remember only the minimal information. Now for each of the B events, we can find the appropriate time window where we need a C to continue. This is shown in panel (c) of the figure. Finally, panel (d) of the figure shows how an occurrence of the episode is recognized. Note that, once we complete an occurrence, we can forget all the extra events we remembered along the way, because we are counting only non-overlapped occurrences. This gains us a lot of memory efficiency.

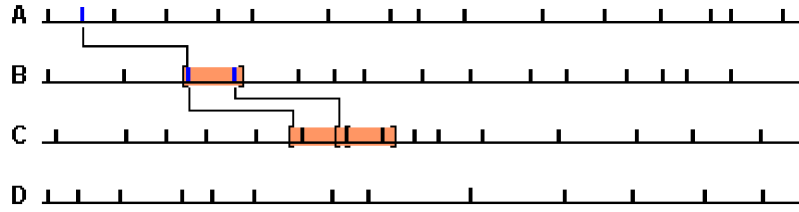
Though the above explanation considered only serial episodes, similar method also works for discovery of other types of episodes as well as other types of temporal constraints [26, 5].



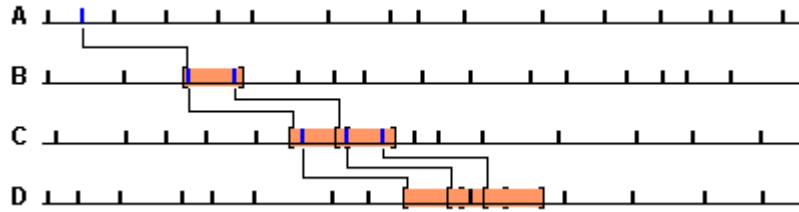
(a) Event Sequence



(b) Step - 1



(c) Step - 2



(d) Step - 3

Figure 2: Frequent serial Episode discovery - Counting Algorithm. Various steps in recognizing an occurrence of a serial episode $A \rightarrow B \rightarrow C \rightarrow D$ are shown. After seeing A , the first episode, the algorithm looks for occurrences of B within the time window as specified by the inter-event time constraint. The multiple possibilities of B are to be remembered till we find one complete occurrence satisfying all inter-event time constraints. In the algorithm, we have to be simultaneously looking for such occurrences for a whole set of episodes through a single pass over the data. See text for more explanation.

4 Algorithms for discovering frequent episodes under temporal constraints

In this section we describe our algorithms that discover frequent episodes under expiry and inter-event time constraints.¹ Since algorithms for taking care of expiry time are available in case of serial episodes [26], we consider the case of only parallel episodes under expiry time constraint. The inter-event time constraints are meaningful only for serial episodes and that is the case we consider. Conceptually, all the algorithms essentially use finite state automata for recognizing episode occurrences, which is similar to the schemes used in [3, 4]. We essentially use the same data structures as in those algorithms for keeping track of potential state transitions of different automata. As already stated, the method is a two step procedure consisting of candidate generation and counting frequencies of a set of candidates. This is shown in *Algorithm 1*.

Algorithm 1 Mining Frequent Episodes

- 1: Generate an initial set of (1-node) candidate episodes (N=1)
 - 2: **repeat**
 - 3: Count the number of occurrences of the set of (N-node) candidate episodes in one pass of the data sequence
 - 4: Retain only those episodes whose count is greater than the frequency threshold and declare them to be frequent episodes
 - 5: Using the set of (N-node) frequent episodes, generate the next set of (N+1-node) candidate episodes
 - 6: **until** There are no candidate episodes remaining
 - 7: Output all the frequent episodes discovered
-

4.1 Parallel episodes with expiry

In this section we present an algorithm that counts the number of non-overlapped occurrences of a set of parallel episodes in which all the constituting events occur within time T_x of each other. In order to ensure that we count the maximum number of occurrences that satisfy the expiry constraint, we need to count the inner most occurrences of each episode. The algorithm here discovers parallel episodes with non-repeated event types. The pseudo-code for the algorithm is

¹This section contains technical details of the counting algorithms and it is assumed that the reader is familiar with such data mining methods. This section can be skipped without any loss of continuity.

listed as *Algorithm 2* in the Appendix.

The algorithm takes as input, the set of candidate episodes, the event sequence and the frequency threshold, and outputs the set of frequent episodes. An occurrence of a parallel episodes requires all its constituent nodes to appear in the event sequence in any order. At any given time, one needs to wait for all the nodes of the episode that remain to be seen. Thus, in an automaton based algorithm for recognizing occurrences, the states of the automaton would denote sets of event types. In the implementation of the algorithm here, instead of a single automaton waiting for for a set of event types, we maintain separate entries for each distinct event type of the episode using a *waits(.)* list indexed by event types. For each event type A , each entry in the list *waits(A)* is of the form $(\alpha, count, init)$, where α is an episode waiting for an A , “*count*” takes values 1 or 0 depending on whether an event of this type (A) has been seen or not, and *init* indicates the latest time of occurrence of this event type.

In *Algorithm 2*, when an event type is seen, we update the *init* field of each entry waiting for it with the current time and retain the entries in the *waits* list. These entries are still waiting for their corresponding event types. When we see the same event type again, we update the *init* field of each of the entries in the *waits* list as earlier. This strategy ensures that all the entries for a given parallel episode remember only the latest occurrences of their corresponding event types. Thus, we effectively track the inner most occurrence.

An occurrence of an episode is complete when there is no entry for an episode which has yet to see the first occurrence of its event type and all the event times (remembered by *init* field) occur within T_x of each other. An episode specific *counter* is used to keep track of the event types already seen. The span of the episode is the difference between the smallest and largest *init* times of the event types for the episode. If the span is within the expiry time T_x , the episode count is incremented and all the entries (in the *waits(.)* lists) for the episode are reinitialized.

If the expiry check fails, we cannot reject all the events types of a parallel occurrence. This is because, in an occurrence of a parallel episode, the constituent event types can occur in any order in the event stream. Only those event types which have occurred before $(t_i - T_x)$, should be rejected, where t_i is the time of the latest event type seen by the algorithm. Effectively, any later

occurrence of these events could possibly complete the parallel episode (without violating the temporal constraint). When an occurrence of α is complete, $\alpha.freq$ is incremented, $\alpha.counter$ is reset and all the entries for the episode are reinitialized.

Candidate generation

The candidate generation scheme is very similar to the one presented in [27] for itemsets. Let α and β be two k -node frequent episodes having $(k - 1)$ nodes identical. The potential $(k + 1)$ -node candidate is generated by appending to α the k^{th} node of β . This new episode is declared as a $(k + 1)$ -node candidate if all its k -node subepisodes are already known to be frequent.

4.2 Serial Episode with Inter-event Constraints

Under an inter-event time constraint, the time of successive events in any occurrence have to be in a prescribed interval. To take care of this we use a new episodes structure. The episode structure now consists of an ordered set of intervals besides the set of event types. An interval $(t_{low}^i, t_{high}^i]$ is associated with i^{th} pair of consecutive of event types in the episode. For example, a 4-node serial episode is now denoted as follows:

$$(A \xrightarrow{(t_{low}^1, t_{high}^1]} B \xrightarrow{(t_{low}^2, t_{high}^2]} C \xrightarrow{(t_{low}^3, t_{high}^3]} D) \quad (2)$$

In a given occurrence of episode $A \rightarrow B \rightarrow C \rightarrow D$ let t_A, t_B, t_C and t_D denote the time of occurrence of corresponding event types. Then this is a valid occurrence of the serial episode with inter-event time constraint given by (2), if $t_{low}^1 < (t_B - t_A) \leq t_{high}^1, t_{low}^2 < (t_C - t_B) \leq t_{high}^2$ and $t_{low}^3 < (t_D - t_C) \leq t_{high}^3$.

In general, an N -node serial episode is associated with, $N - 1$ inter-event constraints of the form $(t_{low}^i, t_{high}^i]$. The algorithm we present is for generalized inter-event constraints. The user needs to specify only the granularity of search by providing a set of non-overlapped time intervals to serve as candidate inter-event time intervals. Using a proper candidate generation scheme and the counting algorithm, we can discover frequent episodes along with the set of most appropriate inter-event intervals for each episode. This algorithm is easily particularized to the case where inter-event time constraints are explicitly specified.

4.2.1 Candidate generation scheme

The generalized inter-event time constraints are a part of the episode structure. In the data sequence, if episode $(A \xrightarrow{(0,5]} B \xrightarrow{(5,10]} C)$ is frequent, the sub-episodes $(A \xrightarrow{(0,5]} B)$ and $(B \xrightarrow{(5,10]} C)$ are also as frequent, but pairing event type A with C we would get $(A \xrightarrow{(? , ?]} C)$ as an episode whose inter-event constraints are not intuitive. Hence, the Apriori based candidate generation is not suitable here.

The candidate episodes in this case are generated as follows. Let α and β be two k -node frequent episodes such that by dropping the first node of α and the last node of β , we get exactly the same $(k - 1)$ -node episode. A candidate episode γ is generated by copying the k -event types and $(k - 1)$ -intervals of α into γ and then copying the last event type of β into the $(k + 1)^{th}$ event type of γ and the last interval of β to the k^{th} interval of γ . Fig. 3 shows the candidate generation process graphically.

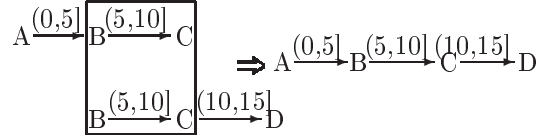


Figure 3: Visualization of Candidate generation for serial episodes with inter-event constraints

4.2.2 Counting episodes with generalized inter-event time constraint

As already stated, the constraints are in the form of intervals $(t_{low}^i, t_{high}^i]$, in which the inter-event times must lie. We first explain the need for a new algorithm to count occurrences of serial episode with this generalized structure. Consider the event sequence

$$\langle (A, 1), (A, 2), (B, 4), (A, 5), (C, 10), (B, 12), (C, 13), (D, 17) \rangle. \quad (3)$$

Let the serial episode under consideration be $(A \xrightarrow{(0,5]} B \xrightarrow{(5,10]} C \xrightarrow{(0,5]} D)$. All the current algorithms for counting occurrences of serial episodes either look at left most occurrence of episode or inner most occurrence of episode (See [26] for details). In the given event sequence, the left most occurrence is $\langle (A, 1), (B, 4), (C, 10), (D, 17) \rangle$ and the inner most occurrence is $\langle (A, 5), (B, 12), (C, 13),$

$(D, 17)$), where as the occurrence $((A, 2), (B, 4), (C, 13), (D, 17))$ alone satisfies the inter-event interval constraints.

The counting algorithm is listed as Algorithm 2 in the Appendix. The algorithm presented uses *waits* lists indexed by event types and a linked list of *node* structures for each episode as the basic data-structures. The entries in the *waits* lists are *nodes*. For each episode we have a doubly inked list of *node* structures with a *node* corresponding to each of the event types and arranged in the same order as that of the episode. The *node* structure has a *tlist* field that stores the times of occurrence of the event-type represented by its corresponding *node*. For example, in the event sequence given by (3), the *node* representing A , after $t = 5$, would have $tlist = \{(A, 1), (A, 2), (A, 5)\}$. Other field in the *node* structure is *visited*, which is a boolean field that indicates whether the event type is seen atleast once.

On seeing an event type E_i , the algorithm iterates over list $waits(E_i)$ and updates each *node* in the list. We explain the procedure for updating the *nodes* by considering the the example sequence given in (3) and the episode $\alpha = (A \xrightarrow{(0,5]} B \xrightarrow{(5,10]} C \xrightarrow{(0,5]} D)$. Working of the algorithm in this example is illustrated in Fig. 4.

The *waits* lists are initialized by adding the *nodes* corresponding to first event type of each episode in the set of candidates to the corresponding $waits(\cdot)$ list. In the example, let the *node* tracking event type A be denoted by $node_A$, and so on. Initially $waits(A)$ contains $node_A$. (That is, the algorithm is waiting for an occurrence of event type A in the data stream). The boxes in Fig. 4 represent an entry in the *tlist* of a *node*. An empty box is one that is waiting for the first occurrence of an event type. On seeing $(A, 1)$, it is added to *tlist* of $node_A$, and $node_B$ is added to $waits(B)$. At any time, *the node structures are waiting for all event types that have been already seen and the next unseen event type*.

The algorithm is now waiting for an occurrence of a B and an A as well. At $t = 4$, the first occurrence of a B is seen. The *tlist* of $node_A$ is traversed to find atleast one occurrence of A , such that $t_B - t_A \in (0, 5]$. Both $(A, 1)$ and $(A, 2)$ satisfy the inter-event constraint and hence, $(B, 4)$ is accepted into the $node_B.tlist$. The rule for accepting an occurrence of an event type (which is not the first event type of the episode) is that *there must be atleast one*

occurrence of the previous event type (in this example A) which can be paired with the occurrence of the current event type (in this example B) without violating the inter-event constraint. Note that this check is not necessary for the first event of the episode. After seeing the first occurrence of B , $node_C$ is added to $waits(C)$. Using the above rules the algorithm accepts $(A, 5)$, $(C, 10)$ into the corresponding $tlists$. At $t = 12$, for $(B, 12)$ none of the entries in $node_A.tlist$ satisfy the inter-event constraint for the pair $A \rightarrow B$. Hence $(B, 12)$ is not added to the $tlist$ of $node_B$. Rest of the steps of the algorithm are illustrated in the figure.

If an occurrence of event type is added to $node.tlist$, it is because there exist events for each event type from the first to the event type corresponding to the $node$, which satisfy the respective inter-event time constraints. An occurrence of episode is complete when an occurrence of the last event type can be added to the $tlist$ of the last $node$ structure tracking the episode.

The $tlist$ entries shown crossed out in the figure are the ones that can be deallocated from the memory. This is because, given the inter-event constraint, they can no longer accept an occurrence of the next event type. In the example, at $t = 12$, when the algorithm tries to insert $(B, 12)$ into $node_B.tlist$, the list of $tlist$ entries for occurrences of A 's is traversed. $(A, 1)$ with inter-event constraint $(0, 5]$ can no longer be paired with a B since the inter-event time duration for any incoming event exceeds 5, hence $(A, 1)$ can be safely removed from the $node_A.tlist$. This holds for $(A, 2)$ and $(A, 5)$ as well. In this way the algorithm frees memory wherever possible without additional processing burden.

In order to track episode occurrences we need to store sufficient back references in data structures to back track each occurrence. This adds some memory overhead, but tracking may be useful in visualizing the discovered episodes.

5 Results

In this section we present some results obtained with our algorithms for analysing spike-train data. We present results both on synthetic data generated through a simulation model as well as on data gathered from experiments on neural cultures. The main reason for using simulator-generated data is that here we can have control on the kind of patterns that the data contains and can thus check whether our algorithms discover the ‘true’ patterns. The simulation model is

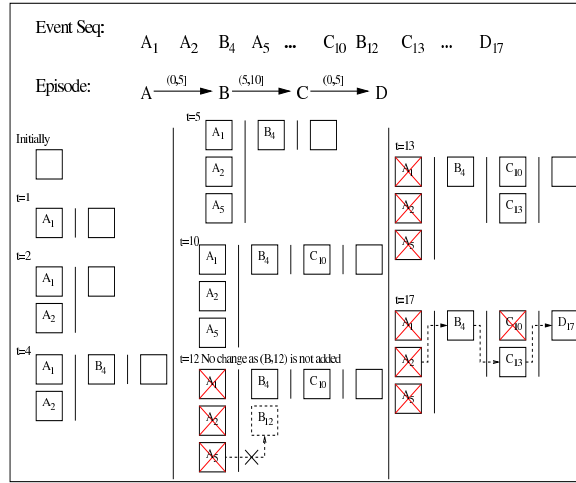


Figure 4: Visualization of Algorithm 3

intended to generate fairly realistic spike trains. For this we actually simulate a network of neurons where each neuron is modelled as a Poisson process whose rate changes with the input received by the neuron. The network would contain random interconnections (which contribute to background spiking) as well as some extra strong interconnections among neurons which will contribute to some correlated firings by groups of neurons. On simulator-generated data we present results to show that our algorithms can discover different types of embedded patterns. We also present some empirical results to argue that the patterns discovered would be statistically significant. We then present results on one set of data gathered through Calcium imaging techniques and on another set of data gathered through multielectrode array experiments.

5.1 The spike data generation model

For the data generation, we use a simulator where each neuron is modelled as an inhomogeneous Poisson process (whose rate varies with time). In the following paragraphs we shall explain the working of our model.

5.1.1 Simulating Arrivals

The number of Poisson arrivals in time Δt is given by

$$P[N(t) - N(t - \Delta t) = k] = \frac{e^{-\lambda(t)\Delta t} (\lambda(t)\Delta t)^k}{k!} \quad (4)$$

Our simulation is conducted in intervals of Δt . Hence the duration of simulation, T , is divided into n non-overlapping intervals each of size Δt . Let the i^{th} interval (i.e. $[i\Delta t, (i+1)\Delta t)$) be denoted by Δt_i . It is assumed that the arrival rate remains constant over this period (i.e. $\lambda(t) = \lambda_i, t \in \Delta t_i$). In a given interval Δt_i , the inter-arrival times are exponentially distributed $\approx \exp(\lambda_i)$. The arrivals in the i_{th} interval are simulated as follows.

$$\text{Arrivals in the interval } \Delta t_i = \{t_i^1, t_i^2, \dots, t_i^{K_i}\}, \forall i \in \{1, \dots, n\} \quad (5)$$

where each t_i^j is defined as follows

$$t_i^j = t_i^{j-1} + \exp(\lambda_i), \forall j \in \{1, \dots, K_i\} \quad (6)$$

and

$$t_i^0 = i\Delta t, t_i^{K_i} \leq (i+1)\Delta t \quad (7)$$

Hence K_i 's are poisson distributed according to equation 4. That is

$$P[K_i = k] = \frac{e^{-\lambda_i \Delta t} (\lambda_i \Delta t)^k}{k!} \quad (8)$$

5.1.2 Network Inter-connection

Our simulation setup consists of a set of N neurons. These neurons are interconnected and a weight is assigned to each inter-connection. Whenever a neuron fires, it injects a weighted input into the neurons that it feeds into. The inter-connections are setup in such a way that the input from a firing neuron will reach a receiver neuron after a certain delay. Each inter-connection is capable of having its own delay. Since the simulation is carried on in steps of Δt , it makes sense to have these delays as whole number multiples of Δt .

In order to generate noise firings, we randomly interconnect neurons. We provide three different schemes for connecting neurons. In the first scheme, for a given neuron a number between 0 and N is randomly chosen. Let this number be k , then k neurons other than the one in consideration, are again randomly picked (with uniform probability) to be the receiver neurons.

In the second scheme, a pair of neurons (n_i, n_j) is picked and with probability 0.5 it is decided whether to have a connection from n_i to n_j . The number inter-connections is, thus, binomially distributed with parameters $(N, p = 0.5)$. The

last scheme consists of connecting all pairs of neurons and we call this the fully inter-connected network.

In all the three schemes of inter-connection, the weight of a connection is a number drawn uniformly from the interval $[-c, c]$.

5.1.3 Injecting patterns

When we want to embed any specific pattern, then, we set the weights of the required connections between neurons to a higher value. For example, if we wish to embed the pattern $A \rightarrow B \rightarrow C$, we would assign higher positive weights to connections $A \rightarrow B$ and $B \rightarrow C$. We shall explain the rational behind the actual weights that we choose in the next section.

5.1.4 Determining the firing rate of a neuron

As stated earlier the simulation is carried on in steps of Δt . Hence the firing rate of a neuron is determined at the start of each Δt interval and is assumed to remain constant over the interval. For random inter-connections the weights are chosen uniformly from the interval $[-c, c]$. The weights for causative inter-connections are assigned as follows. Let E_{strong} be defined as *the probability of firing atleast one spike in Δt upon receiving one input spike from a strong input connection*. The simulator takes E_{strong} as in input and determines the weight for a strong connection as follows.

$$P(N(t + \Delta t) - N(t) > 1) = 1 - P(N(t) - N(t - \Delta t) = 0) \quad (9)$$

$$E_{strong} = 1 - \frac{e^{-\lambda_m \Delta t} (\lambda_m \Delta t)^0}{0!} \quad (10)$$

$$\lambda_m = \frac{-\log(1 - E_{strong})}{\Delta t} \quad (11)$$

Here λ_m is the firing rate required to achieve the desired probability of firing atleast one spike in Δt (i.e. E_{strong}). However due to an absolute refractory period $T_{refractory}$ the number of firings in Δt is actually much less than $\lambda_m \Delta t$.

Let the firing rate of the j^{th} neuron in Δt_i intervals be λ_{ji} . This is determined by the following equation.

$$\lambda_{ji} = \frac{\lambda_m}{1 + e^{(-\Delta \lambda \cdot I_{ji} + d)}} \quad (12)$$

where $I_{ji} = \sum w_{kj} O_k(\hat{i})$, w_{kj} is the weight of the connection from k^{th} to j^{th} neuron and $O_k(\hat{i})$ is the number of spikes fired by k^{th} neuron in $\Delta t_{\hat{i}}$. Note that $(i - \hat{i})\Delta t$ is the delay or time taken for a spike to reach neuron j from neuron k . Here d is a displacement factor set such that with zero input the firing rate of a neuron is λ_{normal} . And $\Delta\lambda$ determines the slope of the sigmoid function. It is currently set to 1.0.

$$\lambda_{normal} = \frac{\lambda_m}{1 + e^{(0+d)}} \quad (13)$$

$$d = \log\left(\frac{\lambda_m}{\lambda_{normal}} - 1\right) \quad (14)$$

Now we set the weight of a strong causative inter-connections such that a single input spike achieves a firing rate of $\beta\lambda_m$ where β is chosen close to 1 (i.e. ≈ 0.9).

$$\beta\lambda_m = \frac{\lambda_m}{1 + e^{(-\Delta\lambda.w_{strong}.1+d)}} \quad (15)$$

$$e^{-\Delta\lambda.w_{strong}.e^d} = \frac{1 - \beta}{\beta} \quad (16)$$

$$(17)$$

Therefore,

$$w_{strong} = \frac{\log\left(\frac{\beta}{(1-\beta)}\left(\frac{\lambda_m}{\lambda_{normal}} - 1\right)\right)}{\Delta\lambda} \quad (18)$$

5.1.5 Adjusting the noise firing rates of neurons in a pattern

When we embed a pattern by having large-weight interconnection between some pairs of neurons, all the neurons that are part of the pattern would have their firing rates increased again and again and thus their average firing rate would be higher than that of others. This would mean that if we look at the histogram of number of spikes by each neuron, we can easily guess which are the neurons that participate in the patterned connections. Since our primary motivation here is to show the effectiveness of our algorithms in discovering hidden patterns, we make a slight modification to the above simulation model to make the discovery problem more difficult. We set the normal firing rate λ_{normal} of all the neurons that are part of a pattern except the first neuron according to eq.(19).

$$\lambda_{adjusted} = \alpha\lambda_{normal}(1 - E_{strong}) \quad (19)$$

where, $\alpha(\approx 1.5)$ is a scaling factor. This rate is achieved by changing the value of d in eq.(12) for the neurons that are part of an embedded pattern. This way, the histogram of spikes by different neurons turns out to be almost flat thus giving no indication of the embedded patterns.

5.1.6 Refractory Period

In this simulation model an absolute refractory period $T_{refractory}$ is used. After a neuron has put out a spike at time t , it is not allowed to fire in the interval $[t, t + T_{refractory})$. $T_{refractory}$ is usually set to a value close to that of Δt .

5.1.7 Simulated Data

We use the model to generate data with different patterns as follows. Let N denote the total number of neurons in the system. (We have generated data with $N=26, 64$ and 100). First we randomly interconnect the neurons using one of the schemes described in section 5.1.2. The weight attached to each synapse is set randomly using a uniform distribution over $[-c, c]$. (We have used $c = 0.50, 0.75$). When we want to embed any specific pattern, then, we set the weights of the required connections between neurons to a higher value. The kind of patterns embedded are explained later.

We set the parameters of the model as follows. The number of neurons, N and the range of weights for random interconnections c , are varied as stated earlier. We choose the firing rate of neurons under no input, say, λ_{normal} . (This represents the noise level for the spiking data). When we embed a pattern, we want some neurons to cause other neurons to fire. This is achieved by increasing their firing rate. For this, we first choose a number, $E_{strong} \in [0, 1]$, which gives the probability that the receiving neuron would generate atleast one spike in the next Δt interval if it receives the expected pattern input. The value of E_{strong} then determines the firing rate λ_m that the neuron should have (by using the Poisson distribution). We then determine the weight of connection needed so that if each of the intended input neurons sends out one spike (in the appropriate time interval) then the receiving neuron would reach close to the firing rate of λ_m under our chosen sigmoidal function.

For the simulations discussed here, we used the following values for parameters: $\lambda_{normal} = 20Hz$, $E_{strong} = 0.95$. (Recall that E_{strong} determines λ_m

which in turn determines weights for the patterned connections). We have chosen $\Delta T = 1$ milli sec and chosen the refractory period ($T_{refractory}$) also the same. (This would mean that in any Δt interval there would be at most one spike from any neuron). We have chosen inter-connection delay $5\Delta t$ which implies a synaptic delay of 5 milli sec.

The patterns we want to embed are the kind shown in Fig. 1. These are realizable by essentially two types of pattern dependent interconnections between neurons. One is where a neuron primes one (as in a serial episode) or many (as in a parallel episode) neurons. Here the weight is determined by requiring that one spike (in the appropriate interval) by the priming neuron would increase the firing rate of the receiving neuron to λ_m so that in the next Δt interval the receiving neuron spikes atleast once with probability E_{strong} . The other kind of interconnection is where many neurons together prime one neuron (which is used in Synfire chains). Here, the weight of each connection is set in such a way that only if each of the input neurons spikes once in the appropriate interval then the firing rate of the receiving neurons would go upto λ_m . (If only a few of the input neurons fire, then the firing rate of the receiving neuron goes up but not all the way upto λ_m).

The weights of random connections are set using a mean-zero distribution and hence, in an expected sense all neurons keep firing at the ‘noise’ rate of λ_{normal} . However, since the actual input can still assume small positive and negative values, this background firing rate would also be fluctuating around λ_{normal} . Since all firings are stochastic, even when a pattern is embedded, the entire patterned firing sequence will not always happen. Also, within a pattern of firing of neurons (as per the embedded pattern), there would be other neurons that would be spiking randomly. *Also, due to our implementing of refractory period, the actual firings of neurons are not Poisson.*

5.2 Discovering patterns in the simulated spike trains

In this section we present some results to illustrate the effectiveness of our datamining algorithms in discovering patterns in spike data. We show that a combination of parallel and serial episodes with appropriate temporal constraints can capture most of the interesting patterns in spike data. We used the simulator described earlier to generate the data. The types of interconnections

among neurons that we used to generate data with different embedded patterns are shown in fig. 1.

As explained earlier, synchronous firing patterns are well described by parallel episodes. To embed a synchrony pattern in the spike data, we use the interconnection scheme given in fig. 1(a). Here neuron A has strong connections into neurons B, C, D . Thus, a spike from A would cause, after a synaptic delay, the other neurons to spike. Because of the way we choose weights for such pattern-based interconnections, this means that with a high probability B, C and D would all fire within one Δt (which is 1 milli sec here) interval. Hence we can discover such patterns by using the method for discovering parallel episodes with an expiry time of less than 1 milli sec. We refer to the circuit shown in the figure as a parallel episode of size 3 (because it involves synchronous firing of three neurons). We can similarly create larger patterns of synchrony.

To create spike data with ordered firing patterns, we use the interconnection scheme similar to the one shown in fig. 1(b). Here, a series of neurons are connected through high weights. As explained earlier, serial episodes capture such patterns. Hence, to discover patterns of ordered firings, we use algorithm for discovering frequent serial episodes with inter-event time constraints. Since we have chosen synaptic delay to be 5 milli sec and use 1 milli sec windows for gathering input into neurons, we can typically use an inter-event interval of 4 – 6 milli sec as the constraint.

To create data with synfire chains, we use the interconnection scheme as illustrated in fig. 1(c). Here, (BCD) , $(FGHI)$ etc are synchronous patterns that are strung together in a tight temporal order. The fixing of weights in this connection scheme is as explained in the previous subsection. Essentially, firing of A would send strong inputs into each of B, C, D . With a high probability they fire synchronously, that is within a window of 1 milli sec. The weights from B, C, D to E are such that only if, in fact, they fire synchronously then with a high probability E would fire thus triggering the next synchrony. We also note here that E would fire within 4 – 6 milli sec of the synchronous firing of (B, C, D) because there is a synaptic delay involved here.

We can discover such patterns as follows. We first discover all (frequent) parallel episodes with expiry time of 1 milli sec or less. This would capture the synchrony patterns. Then for each such parallel episode, we take each of the

occurrences of the episode counted by our algorithm and replace all these events (spikes) with a single event with a new name whose time of occurrence is put as the midpoint of the corresponding occurrence span of the parallel episode. Now on this modified data stream we discover serial episodes with inter-event time constraint of 4 – 6 milli sec. Such a procedure can discover patterns in the form of Synfire chains.

We first show that our method can discover specific network patterns that are embedded in the data generation process. We also illustrate the ability of our method to automatically discover inter-event time constraints most appropriate given the data. We discuss three examples for this.

Example 1

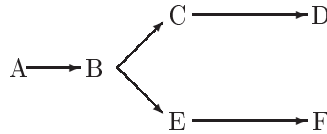


Figure 5: Network pattern for Example 1

In a 26 neurons network (where each neuron corresponds to an alphabet) we embed the pattern shown in Fig.5. The simulation is run for 50 sec and approximately 25,000 spikes are generated. The synaptic delay is set to be about 5 milli sec. We have chosen $\Delta t = 1$ milli sec and have taken refractory time also to be the same.

Episode expiry	Freq. Th.	Time (sec)	Size (No.)	Patterns Discovered
0.0001	0.01	0.23	1(26)	no episode of 2 or more nodes
0.001	0.01	0.29	2(2)	E C : 799; F D : 624
0.002	0.01	0.28	2(2)	E C : 804; F D : 643
0.007	0.01	0.37	2(2)	F E D C : 615

Table 1: Parallel episodes dicovered with different expiry time constraints in Example 1

The sequence is then mined for frequent parallel episodes with different expiry times. The results are given in Table 1. The table shows the expiry time used, the frequency threshold, time taken by the algorithm on a Intel dual core

Inter-event interval	Freq. Th.	Time (sec)	Size (No.)	Patterns Discovered
0.000-0.001	0.01	0.29	2(4)	C E : 410; E C : 400 D F : 329; F D : 303
0.000-0.002	0.01	0.31	2(4)	C E : 422; E C : 408 D F : 348; F D : 323
0.002-0.004	0.01	0.26	1(26)	no 2 or more node episodes
0.004-0.006	0.01	0.29	4(4)	A B C D : 597 A B E F : 589 A B E D : 530 A B C F : 530

Table 2: Serial episodes discovered with different inter-event constraints in Example 1

PC running at 1.6 GHz, the size of the largest frequent episode discovered and the number of episodes of this size along with the actual episodes. We follow the same structure for all the tables in the three examples. The frequency threshold is expressed as a fraction of the entire data length. A threshold of 0.01 over a data length of 25,000 spike events requires an episode to occur at least 250 times before it is declared as frequent. From Table 1 it can be seen that (*CE*) and (*DF*) turn out to be the only frequent parallel episodes if the expiry time is 1 to 2 milli sec. If the expiry time is too small, we get no frequent episodes (at this threshold). On the other hand, if we increase the expiry time to be 7 milli sec which is greater than a synaptic delay, then even (*FEDC*) turns out to be a parallel episode. This shows that by using appropriate expiry time, parallel episodes discovered capture synchronous firing patterns.

The results of serial episode discovery are shown in Table 2. With an inter-event constraint of 4-6 milli sec, we discover all paths in the network (Fig. 5). When we prescribe that inter-event time be less than 2 milli sec (when synaptic delay is 5 milli sec), we get nodes in the same level as our serial episodes. If we use intervals of 2-4 milli sec, we get no episodes because synchronous firings mostly occur much closer and firings related by a synapse have a delay of 5 milli sec. Thus, using inter-event time constraints, we can get fair amount of information of the underlying connection structure. It may seem surprising that we also discover $A \rightarrow B \rightarrow C \rightarrow F$ and $A \rightarrow B \rightarrow E \rightarrow D$ when we use 4–6 milli sec constraint. This is because, the network structure is such that *D* and

F fire about one synaptic delay time after the firing of C and E . Thus, the serial episodes give the sequential structure in the firings which could, of course, be generated by different interconnections. The frequent episodes discovered provide a handle to unearthing the hierarchy seen in the data (i.e. which events co-occur and which ones follow one another).

Example 2

In this example we consider the network connectivity pattern as shown in Fig. 1(c). As stated earlier, this is an example of possible network connectivity that can generate Synfire chains. We use the same parameters in the simulator as in Example 1 and generate spike trains data using this connectivity pattern. Table 3 shows the parallel episodes discovered and Table 4 shows the serial episodes discovered with different inter-event constraints. From the tables, it is easily seen that parallel episodes with expiry time of 1 milli sec and serial episodes with inter-event time constraint of about one synaptic delay, together give good information about underlying network structure. In this example, we illustrate how our algorithms can discover synfire chain patterns. As explained earlier, we first discover all parallel episodes with expiry time 1 milli sec. Then for each frequent parallel episode, we replace each of its occurrences in the data stream by a new event with event type being the name of the parallel episode. This new event is put in with a time of occurrence which is the mean time in the episode occurrence. We then discover all serial episodes with different inter-event time constraints. The results obtained with this method are shown in Table 5. As can be seen, the only pattern we discover is the underlying synfire chain. This example shows that by proper combination of parallel and serial episodes, we can obtain fairly rich pattern structures which are of interest in neuronal spike train analysis.

Episode expiry	Freq. Th.	Time (sec)	Size (No.)	Patterns Discovered
0.001	0.01	0.15	4(1)	L K : 307 C B D : 293 H G F I : 268 rest are sub-episodes

Table 3: Parallel episodes discovered in Example 2

Inter-event interval	Freq. Th.	Time (sec)	Size (No.)	Patterns Discovered
0.002-0.004	0.01	0.157	1(26)	no episodes of 2 or more nodes
0.004-0.006	0.01	0.469	6(24)	A D E H J K : 195 A D E I J K : 194 A D E H J L : 193 A C E H J K : 192
0.006-0.008	0.01	0.156	1(26)	no episodes of 2 or more nodes

Table 4: Serial episodes discovered under different inter-event constraints in Example 2

Inter-event interval	Freq. Th.	Time (sec)	Size (No.)	Patterns Discovered
0.002-0.004	0.01	0.11	1(20)	no episodes of 2 or more nodes
0.004-0.006	0.01	0.14	6(1)	A [C B D] E [H G F I] J [L K] : 137
0.006-0.008	0.01	0.12	1(20)	no episodes of 2 or more nodes

Table 5: Synfire chain episodes discovered in Example 2

Example 3

In this example, we choose a network pattern where different pairs of interconnected neurons can have different synaptic delays and we demonstrate the ability of our algorithm to automatically discover appropriate inter-event intervals. The pattern is shown in Fig. 6, where we have different synaptic delays as indicated on the figure, for different inter-connections.

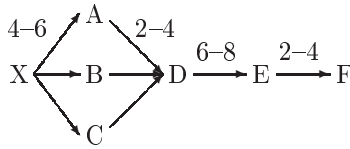


Figure 6: Network Pattern for Example 3

The results for parallel episode discovery (see Table 6) show that (ABC) is the group of neurons that co-spike together. The serial episode discovery

Episode expiry	Freq. Th.	Time (sec)	Size (No.)	Patterns Discovered
0.001	0.01	0.28	3(1)	A B C : 614
0.002	0.01	0.25	3(1)	A B C : 617
0.004	0.01	0.28	4(1)	A B C D : 537
0.006	0.01	0.32	4(2)	X A B C : 602 A B C D : 542

Table 6: Parallel episodes discovered under different expiry times in Example 3

Inter-event interval	Freq. Th.	Time (sec)	Size (No.)	Patterns Discovered
0.000-0.002	0.01	0.32	2(6)	A C : 385; B A : 376 B C : 373; A B : 372 C A : 361; C B : 355
0.002-0.004	0.01	0.37	2(4)	E F : 783; A D : 656 C D : 651; B D : 646
0.004-0.006	0.01	0.28	2(3)	X A : 790; X B : 774 X C : 769
0.006-0.008	0.01	0.29	2(2)	D E : 720; X D : 454

Table 7: Serial Episodes discovered under different inter-event time constraints in Example 3

Inter-event interval	Freq. Th.	Time (sec)	Size (No.)	Patterns Discovered
{0.000-0.002, 0.002-0.004, 0.004-0.006, 0.006-0.008, 0.008-0.010}	0.01	1.37	5(1)	$X \xrightarrow{0.004-0.006} [ABC]$ $\xrightarrow{0.002-0.004} D \xrightarrow{0.006-0.008}$ $E \xrightarrow{0.002-0.004} F : 372$

Table 8: Synfire chain episodes discovered in Example 3

results are given in Table 7. As can be seen from the table, with different pre-specified inter-event time constraints we can discover only different parts of the underlying network graph because no single inter-event constraint captures the full pattern.

As in Example 2, we replace occurrences of parallel episode with a new event in the data stream. We then run Algorithm2 to discover serial episodes along with inter-event constraints, given a set of possible inter-event intervals. The results obtained are shown in Table 8. As can be seen from the table, the algorithm is very effective in unearthing the underlying network pattern.

5.2.1 Performance of algorithms with multiple patterns

The earlier examples clearly demonstrate the ability of our data mining algorithms in unearthing the connectivity pattern in the neuronal network that generated the data. To keep the examples simple we considered only single patterns and on single data sets. Next we demonstrate the performance of the algorithm, averaged over many independently generated random datasets, when multiple patterns of different sizes are present. We illustrate this for all the three types of patterns. We use network with 64 neurons here since most typical micro electrode arrays have 64 channels.

First we consider a 64 neuron system with one or more circuits of synchrony embedded. We have varied the size of the synchrony pattern from 8 to 12 and have experimented with embedding upto four distinct patterns. For each pattern to be embedded, the actual neurons that participate in the pattern are chosen randomly. With such circuits in place we generated many data sets with each data set of 50 sec duration. (Since the normal firing rate is 20 Hz, in 50 sec each neuron would, on the average, spike 1000 times thus giving us a data set of about 60,000 spikes, which is the typical size of spike data sets analyzed).

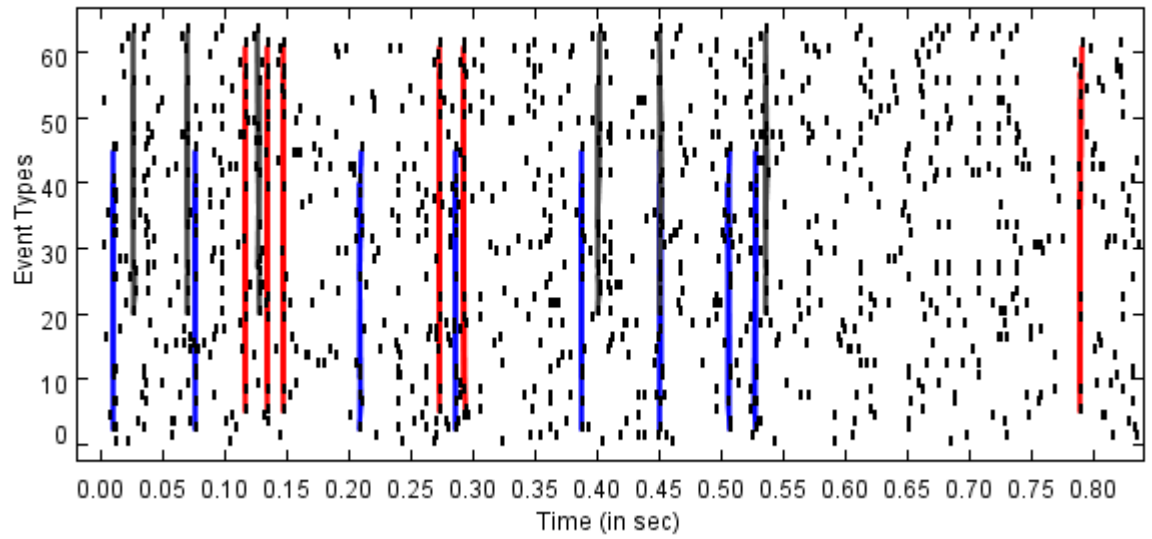
The results of our parallel episode discovery are shown in Table 9. As explained earlier, our algorithm systematically discovers parallel episodes of all sizes whose frequencies are above the threshold set. We have chosen a threshold of 300. (We discuss choosing of the threshold in the next subsection). The first four columns of the table are self-explanatory. The last column shows the percentage of the discovered frequent episodes that are part of the embedded pattern for various sizes. As can be seen from the table, even at size three, all episodes discovered are part of the embedded pattern. Thus, all long synchrony patterns we discover are all ‘correct’ in the sense that they are actually present in the neural system that generated the spike data.

We also like to point out that the time taken by our method to discover all the parallel episodes is only about 30 sec on a PC even for discovering four different synchrony patterns each involving 12 neurons. This illustrates the fact that these algorithms are very efficient in unearthing the patterns.

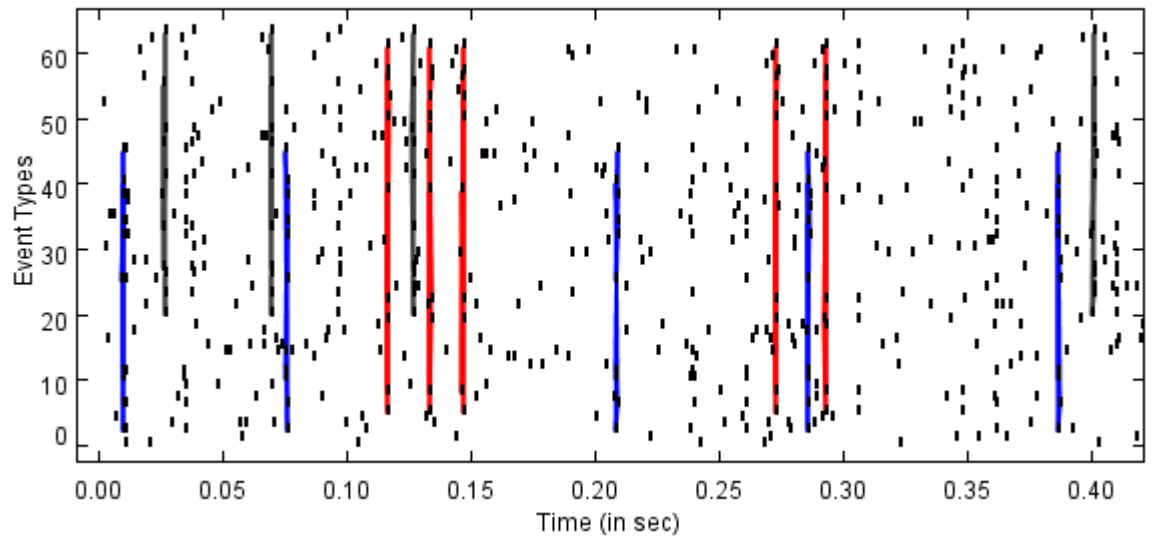
In fig. 7 we show some of the occurrences of three different synchronous firing patterns as a raster plot. We show them in two different windows on the time axis.

Pattern Type	Size	No. of distinct patterns	Time taken (in sec)	Fraction of detected frequent episodes that are part of the embedded pattern			
				Pattern Length	Min Count	% Fraction	
Parallel	8	2	1.968	1	941	25.0%	
				2	785	100.0%	
				8	520	100.0%	
	3	2.438	3	2.438	1	1001	37.5%
					2	841	100.0%
					8	542	100.0%
	4	2.844	4	2.844	1	963	50.0%
					2	812	100.0%
					8	550	100.0%
Parallel	10	2	5.156	1	987	31.2%	
				2	829	100.0%	
				10	507	100.0%	
	3	7.141	3	7.141	1	985	46.9%
					2	829	100.0%
					10	480	100.0%
	4	9.219	4	9.219	1	970	62.5%
					2	823	100.0%
					10	465	100.0%
Parallel	12	2	18.64	1	906	37.5%	
				2	765	100.0%	
				12	408	100.0%	
	3	27.875	3	27.875	1	963	56.2%
					2	802	100.0%
					12	400	100.0%
	4	37.578	4	37.578	1	929	75.0%
					2	785	100.0%
					12	389	100.0%

Table 9: Discovery of Synchronous firing patterns: Averaged results over 100 datasets for discovering parallel episodes of different sizes with multiple patterns embedded. The first three columns show type of pattern, number of distinct patterns embedded and time taken on one dataset. When we embed a pattern of size, say, 8, the algorithm would discover parallel episodes at all sizes upto 8 in its level-wise iterations. The last column shows the minimum frequency of discovered patterns for these smaller sizes and also the fraction of discovered episodes of that size which are part of the embedded pattern.



(a)



(b)

Figure 7: Some of the occurrences of the synchronous firing patterns in a typical dataset.

We next illustrate discovering ordered firing sequences with tight temporal relationships. We embed many such serial patterns of different sizes to test our method. These results are shown in Table 10. Once again, from the results it is easily seen that the method is very effective in unearthing the patterns of interest. Also, the time taken here is much smaller (less than 3 sec). This is because, the tight inter-event time constraints control the growth of candidate patterns in the frequent episode discovery method.

In fig. 8 we illustrate some of the occurrences of the serial episodes in two different time windows on the data.

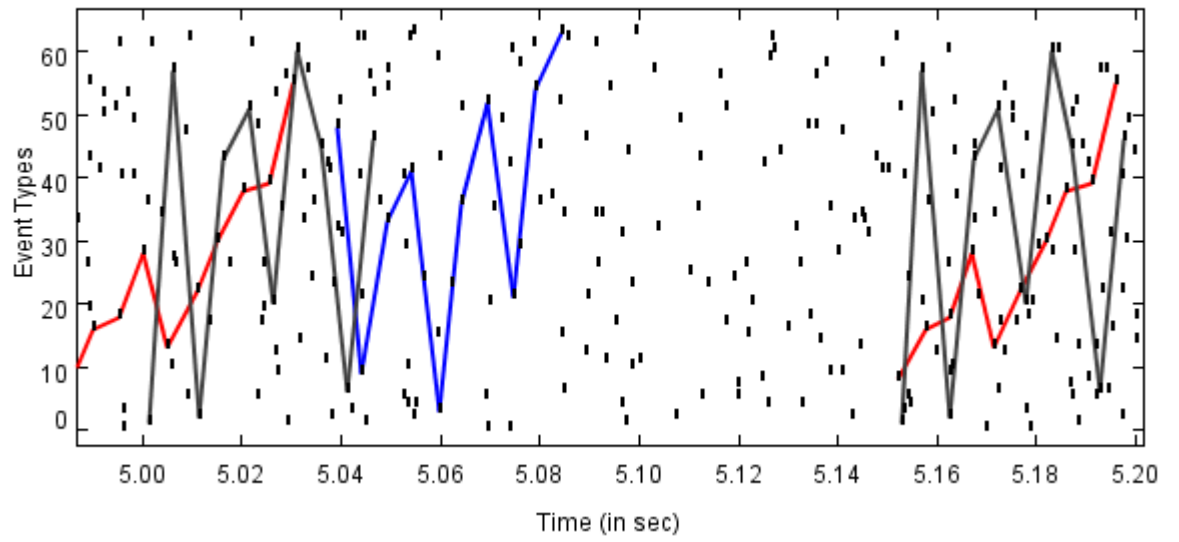
We have conducted similar experiments with multiple synfire chain patterns. Our method is equally effective in discovering Synfire chains. Table 11 shows results obtained when each parallel episode inside the synfire chain has size 4. We have considered 4 and 6 such parallel episodes strung together to make the synfire chain and we have embedded upto 2 such patterns. The table has the same structure as earlier tables and shows the type of synfire chain pattern, number of patterns embedded and the percentage of discovered patterns (of different sizes) which are part of the embedded patterns. Since a synfire chain pattern is composed of parallel episodes and serial episodes on modified data stream, we show the percentage of discovered patterns for these two cases separately. Table 12 shows similar results for the case where each parallel episode in the synfire chain is of size 4. Here we string together 4, 6 or 8 such parallel episodes and we embed upto 3 such patterns. From these tables, it is quite clear that our algorithms are very effective in unearthing synfire chain patterns even when multiple such patterns exist. Fig. 9 shows the discovered Synfire chains in one set of data.

5.3 Assessing significance of frequent episodes discovered

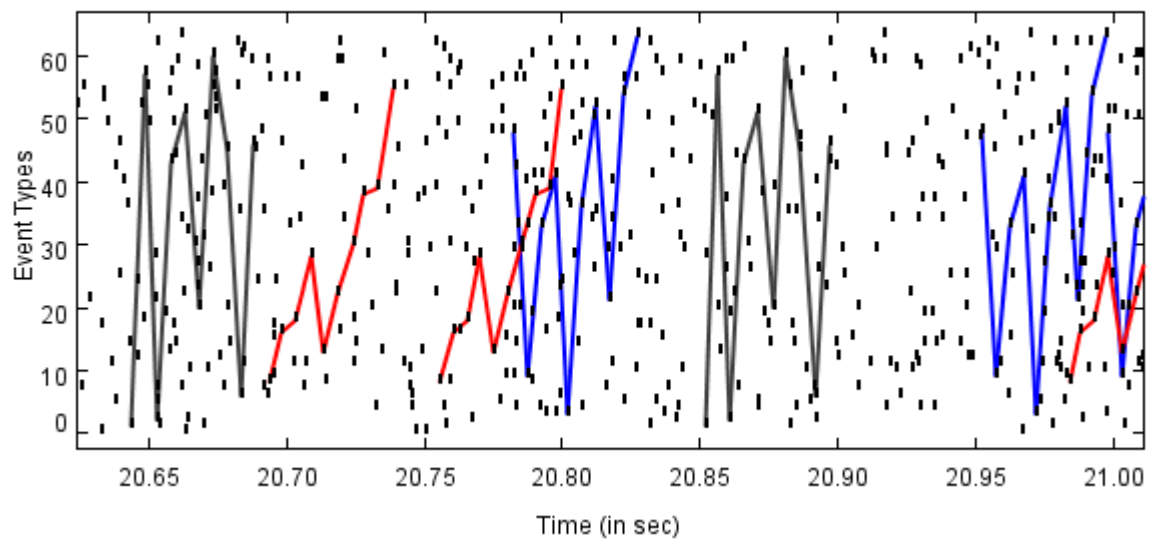
The empirical results presented earlier show that if we generate spike data using special embedded patterns in it then our algorithms can detect them. That is, if the spike data is generated by a system of interconnected neurons with a few strong excitatory connections, then the frequent episodes we discover clearly bring out the connection pattern in the network. However, these results do not answer the question: if the algorithm detects some frequent episodes what confidence do we have that they correspond to some patterns in the underlying

Pattern Type	Size	No. of distinct patterns	Time taken (in sec)	Fraction of detected frequent episodes that are part of the embedded pattern				
				Pattern Length	Min Count	% Fraction		
Serial	8	2	1.766	1	1001	25.0%		
				2	867	100.0%		
				8	426	100.0%		
		3	1.797	4	1.891	1	1000	37.5%
						2	879	100.0%
						8	443	100.0%
		4	1.891	4	1.891	1	957	50.0%
						2	851	100.0%
						8	430	100.0%
Serial	10	2	1.844	1	984	31.2%		
				2	866	100.0%		
				10	377	100.0%		
		3	1.953	4	2.031	1	935	46.9%
						2	817	100.0%
						10	358	100.0%
		4	2.031	4	2.031	1	945	62.5%
						2	817	100.0%
						10	345	100.0%
Serial	12	2	1.922	1	1007	37.5%		
				2	884	100.0%		
				12	311	100.0%		
		3	2.203	4	2.297	1	976	56.2%
						2	853	100.0%
						12	309	100.0%
		4	2.297	4	2.297	1	967	75.0%
						2	849	100.0%
						12	303	100.0%

Table 10: Discovery of ordered firing sequences: Results (averaged over 100 datasets) of discovery of serial episodes with inter-event time constraints when multiple patterns are embedded. The columns in the table are essentially same as those in Table 9.



(a)



(b)

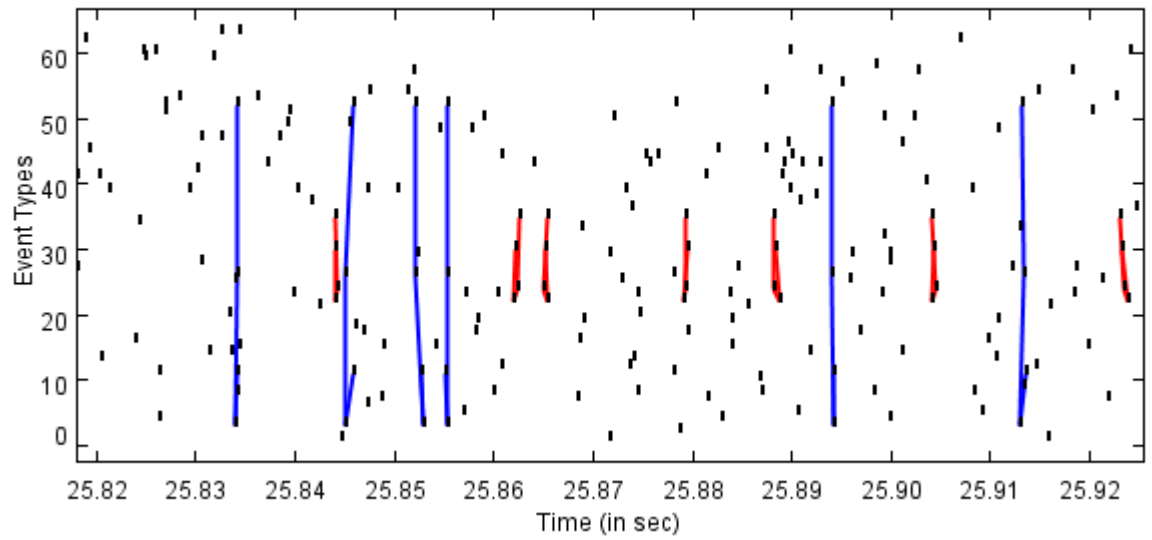
Figure 8: Some occurrences of ordered firing sequences in a typical dataset

Pattern Type	No. of patterns	Episode Type	Time (in sec)	Fraction of frequent episodes that are part of embedded patterns			
				Nodes	Min Count	% Fraction	
Syn-5 1-(5)-1-(5) -1-(5)-1-(5)	1	Parallel	1.042	1	965	31.2%	
				2	799	100.0%	
				5	664	100.0%	
	2	Parallel	1.232	1	955	62.5%	
				2	802	100.0%	
				5	659	100.0%	
	3	Parallel	1.252	1	942	62.5%	
				2	794	100.0%	
				5	667	100.0%	
		1	Parallel	1.162	1	925	46.9%
					2	780	100.0%
					5	635	100.0%
		Serial (mod)	0.631	1	634	30.0%	
				2	580	100.0%	
				12	74	100.0%	

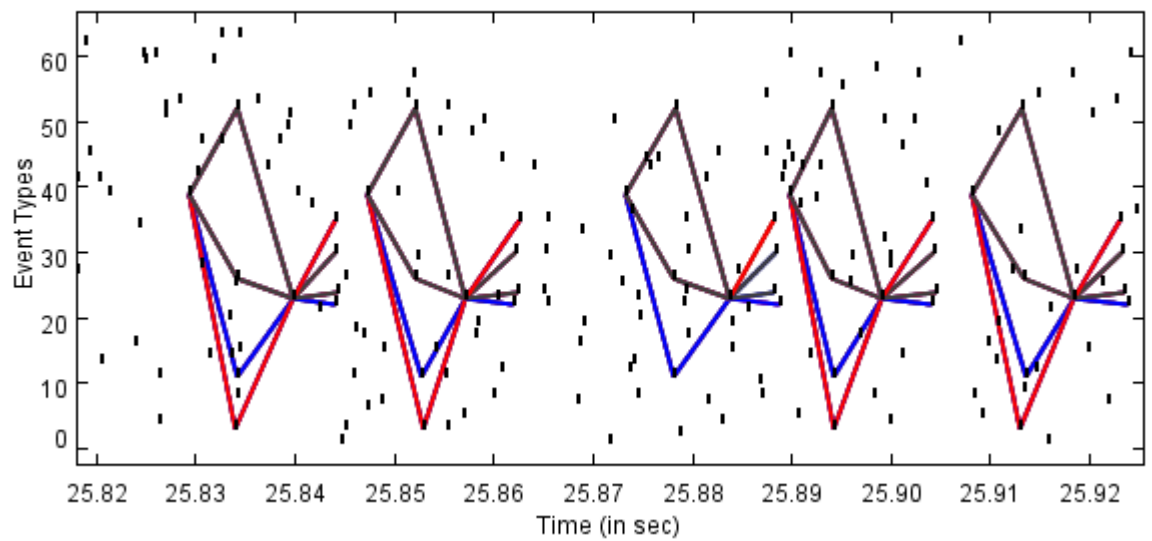
Table 11: Results of discovery for multiple synfire chain patterns. The general structure of the table is similar to the earlier ones. Here all parallel episodes are of size 5. We string together 4 or 6 such parallel episodes to make the synfire chain pattern and this is shown as pattern type in the table. We have used Parallel Episode expiry = 0.001 sec, and Serial Episode Inter-event time constraint = 0.004 to 0.006 sec. The table shows the two phases – parallel episodes and modified serial episodes, separately both for time taken and for the percentage of discovered episodes that are part of embedded pattern.

Pattern Type	No. of patterns	Episode Type	Time (in sec)	Fraction of frequent episodes that are part of embedded patterns		
				Nodes	Min Count	% Fraction
Syn-4 1-(4)-1-(4) -1-(4)-1-(4)	1	Parallel	0.982	1	990	25.0%
				2	848	100.0%
				4	737	100.0%
	2	Parallel	1.032	1	936	50.0%
				2	783	100.0%
				4	697	100.0%
		Serial (mod)	0.561	1	696	40.0%
				2	629	100.0%
				8	226	100.0%
	3	Parallel	1.092	1	925	75.0%
				2	781	100.0%
				4	686	100.0%
Serial (mod)		0.311	1	685	85.7%	
			2	617	100.0%	
			8	232	100.0%	
Syn-4 1-(4)-1-(4) -1-(4)-1-(4) -1-(4)-1-(4)	1	Parallel	1.022	1	949	37.5%
				2	798	100.0%
				4	709	100.0%
	2	Parallel	1.052	1	708	26.1%
				2	630	100.0%
				12	125	100.0%
		Serial (mod)	0.381	1	934	75.0%
				2	777	100.0%
				4	682	100.0%
	Serial (mod)	0.381	1	681	85.7%	
			2	624	100.0%	
			12	111	100.0%	
Syn-4 1-(4)-1-(4) -1-(4)-1-(4) -1-(4)-1-(4) -1-(4)-1-(4)	1	Parallel	1.031	1	936	50.0%
				2	784	100.0%
				4	688	100.0%
	Serial (mod)	0.711	1	687	40.0%	
			2	620	100.0%	
			16	72	100.0%	

Table 12: Discovery of Synfire chain patterns where the parallel episodes are all of size 4. We string together 4, 6 or 8 such parallel episodes to make synfire chain patterns. Structure of table same as the previous one



(a)



(b)

Figure 9: Some occurrences of discovered Synfire chains

neural system. This is a question regarding the statistical significance of the discovered frequent episodes. That is, we need to ask how high should the frequency of an episode be so that, with a high confidence, we can assert that the connectivity pattern implied by the episode is, in some sense, characteristic of the system generating the data.

To answer this question we have to essentially choose a *null hypothesis* that asserts that there is no ‘structure’ in the system generating the data. Then we need to calculate the probability that an episode of a given size would have a given frequency in the data generated by such a model and this will tell us what is the chance of a discovered frequent episode coming up by chance in ‘random’ data and hence tells us the statistical significance of the discovered frequent episodes. This can also allow us to calculate the frequency threshold so that all frequent episodes (with frequency above this threshold) are statistically significant at a given level of confidence. Such an analysis is presented for the case of serial episodes without any temporal constraints under the null hypothesis that the event stream is generated by an *iid* process in [4].

That analysis is not directly applicable for the multineuronal spiking data application because we have temporal constraints on episode occurrences here. But, more importantly, a null hypothesis of an *iid* process generating the spike data is not really attractive here. For example, even if we can reject the null hypothesis that spike trains are produced by independent Poisson processes, it does not mean that the system generating the data has strong correlations or connectivity patterns as indicated by our episodes.

We like to note here that all current methods of spike data analysis, whenever they consider issues of statistical significance, deal with a null hypothesis of *iid* processes generating spike data. One notable exception is the work in [28] where more complicated null hypotheses are considered. However, this work does not deal with finding useful patterns in spike data; the objective of the analysis there is to determine the time scale at which exact times of spikes may carry useful information as opposed to all information being carried by only the spiking frequency.

Here we want to consider a composite null hypothesis in which we include not only *iid* processes, but also other models for interdependent neurons without any specific strong connectivity patterns or strong predispositions for coordinated

firing. It is difficult to capture all such models in an analytically tractable mathematical formulation. Hence, we take the approach of capturing our null hypothesis in a simulation model and estimate the relevant probabilities by generating many random data sets from such a model. (This approach is similar in spirit to the so called ‘jitter’ method [11]).

We generate our random data sets using essentially three different types of models. For the first one, we use the same simulator as described earlier; but we allow only the random interconnections (with weights of interconnections uniformly distributed over $[-c, c]$). This will capture models where the poisson processes representing spikes by different neurons are interdependent (with the firing rate of a neuron being dependent on spikes output by other neurons) but without any bias for some specific interconnectivity pattern or coordinated firing. Next, we generate data sets by assuming that different neurons generate spikes as independent Poisson processes by simply choosing random fixed rates for the neurons. In this, we also include cases where many neurons can have the same firing rate. For this, we fix five or ten different random firing rates and randomly assign each neuron to have one of these firing rates. For our third type of data sets, we include models where rates of firing by neurons change; but without any relation to firing by other neurons. For this we choose random firing rates for neurons and at $50\Delta t$ time steps we randomly perturb the firing rate. Here also we include the case where firing rates of some random subsets of neurons are all tied together.

Thus our null hypothesis includes models where different neurons could be *iid* Poisson processes, or inhomogeneous Poisson processes where the firing rates may be correlated but the rate is not dependent on firing of other neurons. In addition, our null hypothesis also includes models where rates of firing change based on spikes output by other neurons but without any bias for specific strong interconnectivity patterns. We feel that this is a large enough set of models to consider in the null hypothesis. If, based on our episode frequencies, we can reject the null hypothesis, then, it clearly demonstrates that episodes with sufficiently high frequency can not come about unless there is a bias or interdependence in the underlying neural system for coordinated firing by some groups of neurons.

By generating many data sets under the models in our null hypothesis and

calculating frequencies of episodes of different sizes we now show that it is highly unlikely to have long frequent episodes if the data generation model does not have any specific biases.

The specific random data sets are as follows. All data sets are from a 26 neuron system. We generated ten sets of random interconnection weights. In one half of these, the weights are chosen with a uniform distribution over $[-0.5, 0.5]$ and in the other half the weights are uniformly distributed over $[-0.5, 0.5]$. With each set of random weights, we generated ten sets of data (25 000 spikes) by running the simulator with those weights. The normal firing rate (i.e., the rate of firing when input is zero) is set at 20 Hz. Thus we have 100 data sets in which, while neurons fire with input dependent firing rates, there are no special causative connections. We generated another 25 data sets (of 25,000 spikes each) where each neuron had a fixed firing rate chosen from a uniform distribution over $[10Hz, 30Hz]$. In another 25 data sets, we have five different firing rates chosen randomly from the same interval and each neuron is randomly assigned to one of these firing rates. In another 25 data sets we randomly choose a new firing rate for each neuron from the same interval every $50\Delta t$ time units. Here different neurons are independent inhomogeneous Poisson processes. Finally, in another 25 data sets, we randomly divide the neurons into five groups. All neurons in a group would have the same firing rate. The firing rates are updated every $50\Delta t$ time units by choosing from a uniform distribution over the same interval as earlier. Thus, we have a total of 200 data sets. In half of them, the firing rate of any neuron is a function of the actual outputs of other neurons connected to it though all interconnections weights are random with zero mean. Thus, though the neurons are interdependent, there are no biases for any specific connection pattern. In the other half of the data sets the firing rates of neurons are random, fixed or randomly changed, some of the neurons may be correlated in the sense of having the same fixed or varying firing rate, but firing rates are not dependent on outputs of other neurons. We also note here that in all cases we have chosen the random firing rates in such a way that the average firing rate of the total system is roughly same as that in the experiments described in the earlier subsections.

In each of these data sets, We discover serial and parallel episodes (with the usual temporal constraints) of size upto 10 with a frequency threshold of zero

Size	Max. Episode Frequency		
	Avg	Max	Min
1-Node	1084.81	1165.00	1038.00
2-Node	60.21	76.00	54.00
3-Node	6.52	9.00	5.00
4-Node	2.03	3.00	2.00
5-Node	0.06	2.00	0.00
6-Node	0.00	0.00	0.00
7-Node	0.00	0.00	0.00
8-Node	0.00	0.00	0.00
9-Node	0.00	0.00	0.00
10-Node	0.00	0.00	0.00
Sample size = 100			

Table 13: Statistics for parallel episode mining on random spike sequences generated using the model of interdependent neurons with random interconnections. (Parallel Episode Expiry constraint = 0.001 sec). For different sizes of episodes, we show the maximum frequency of any episode of that size. Each entry shows the maximum, minimum and average values of the maximum frequency. These statistics are obtained from a sample size of 100 data sets

so that we get frequencies for all episodes. We then compare the maximum frequencies (averaged over all data sets) of episodes of different sizes obtained from this random data sets to the minimum frequencies observed for same size episodes on data sets with patterns embedded in them. For this comparison we have generated another twenty data sets (using the earlier simulator) where a large episode (serial or parallel as needed) is embedded and the average firing rate is same as that in the random data sets. For the random data case, we show the results as two parts. First part corresponds to the 100 data sets where neurons have spike-input dependent firing rates. The second part corresponds to the 100 data sets where fixed or varying random firing rates are chosen for the neurons.

Tables 13 – 15 show the results obtained in case of parallel episodes. Table 13 shows the maximum observed frequency of episodes for various sizes in case of the random data obtained from our model of interdependent neurons but with random interconnection weights. Table 14 shows the same for the case of data generated using different kinds of random firing rates for neurons as explained earlier. These tables show statistics obtained from a sample size of 100 data sets each. These numbers are to be compared with those in Table 15

Size	Max. Episode Frequency		
	Avg	Max	Min
1-Node	1249.00	1513.00	1004.00
2-Node	76.55	111.00	52.00
3-Node	7.62	12.00	5.00
4-Node	2.12	3.00	0.00
5-Node	0.04	2.00	0.00
6-Node	0.00	0.00	0.00
7-Node	0.00	0.00	0.00
8-Node	0.00	0.00	0.00
9-Node	0.00	0.00	0.00
10-Node	0.00	0.00	0.00
Sample size = 100			

Table 14: Statistics for parallel episode mining on random spike sequences generated using random (fized or varying) firing rates for neurons. (Parallel Episode Expiry constraint = 0.001 sec). For different sizes of episodes, we show the maximum frequency of any episode of that size. Each entry shows the maximum, minimum and average values of the maximum frequency. These statistics are obtained from a sample size of 100 data sets

Size	Min. Episode Frequency		
	Avg	Max	Min
1-Node	978.80	1074.00	933.00
2-Node	822.70	913.00	777.00
3-Node	763.35	853.00	714.00
4-Node	711.20	801.00	664.00
5-Node	657.56	702.00	620.00
6-Node	616.25	671.00	585.00
7-Node	571.50	598.00	543.00
8-Node	537.08	570.00	504.00
9-Node	493.50	525.00	468.00
10-Node	464.88	494.00	433.00
Sample size = 20			

Table 15: Statistics for parallel episode mining on spike sequence data with embedded patterns in it. (Parallel Episode Expiry constraint = 0.001 sec). For different sizes of episodes, we show the minimum frequency of any episode of that size which is a subepisode of the embedded pattern. Each entry shows the maximum, minimum and average values of the minimum frequency. These statistics are obtained from a sample size of 20 data sets

minimum observed frequency of episodes that are part of embedded patterns for different sizes. These numbers are obtained from our simulation model with one large parallel episode embedded. These are statistics obtained from a sample of 20 data sets. Fig. 10 shows the plot of maximum frequencies of episodes in noise sequences and minimum frequency of relevant episodes in sequences with patterns versus episode size. For the plot showing minimum frequencies for the correct episodes in data with patterns, we show the observed variation in minimum frequency as an error bar on the figure.

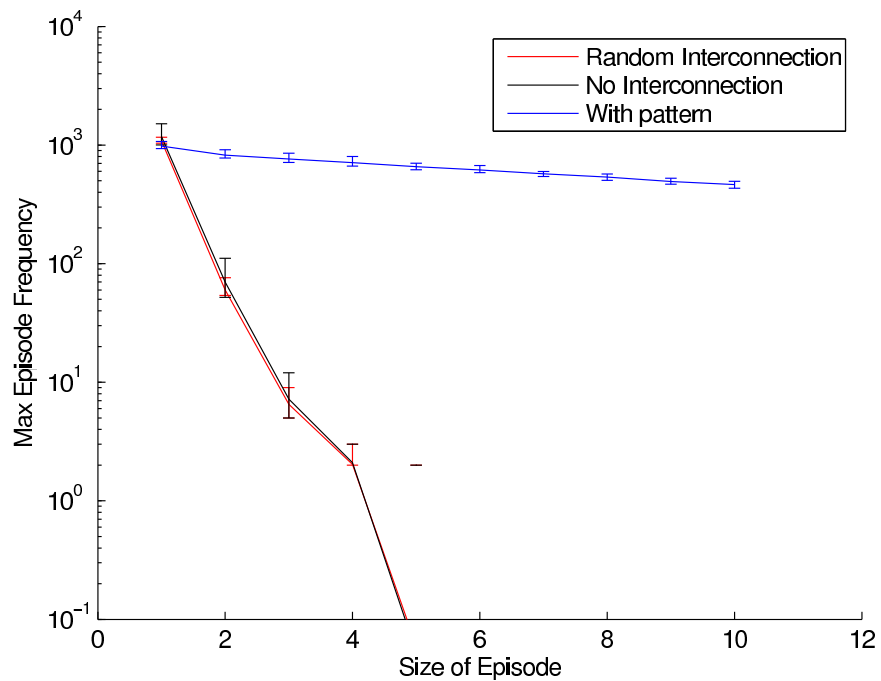


Figure 10: Differences in episode frequencies in noise sequences and sequences with patterns. All are parallel episodes with expiry time constraint of 0.001 sec. For the case of data with patterns, we show minimum frequency for any episode that is part of the embedded pattern and the error bars show the range of variation. The figure clearly shows that it is extremely unlikely to have episodes of size 3 or more with appreciable frequency ‘by chance’.

From the table it can be seen that, even for size 2, the maximum frequency of an episode in the random data is very small. From size 3 onwards, all episodes have frequency less than 10 in the random data. On the other hand, when the data contains patterns, even the minimum observed frequencies of that size

Size	Max. Episode Frequency		
	Avg	Max	Min
1-Node	1084.81	1165.00	1038.00
2-Node	70.51	84.00	59.00
3-Node	9.22	13.00	8.00
4-Node	3.30	4.00	3.00
5-Node	2.02	3.00	2.00
6-Node	1.24	2.00	0.00
7-Node	0.04	2.00	0.00
8-Node	0.02	2.00	0.00
9-Node	0.00	0.00	0.00
10-Node	0.00	0.00	0.00
Sample size = 100			

Table 16: Statistics for serial episode mining on random spike sequences generated using the model of interdependent neurons with random interconnections. (Serial Episode Inter-event time constraint is 0.004-0.006 sec) For different sizes of episodes, we show the maximum frequency of any episode of that size. Each entry shows the maximum, minimum and average values of the maximum frequency. These statistics are obtained from a sample size of 100 data sets

episodes (which are part of the embedded pattern or ground truth) are about two orders of magnitude larger. We also note here that the frequencies of 1-node episodes are comparable in the random and patterned data sets which is due to the fact that we have ensured that the average firing rates of neurons in both sets of data are same. These results provides sufficient statistical justification that it is highly unlikely to have long episodes with appreciable frequencies if the data source does not have the necessary bias.

Tables 16 and 17 show the results obtained for serial episode mining for the two different kinds of random spike sequences as earlier and Table 18 shows the results for serial episode mining on data that contains patterns in it. Once again, it is seen that in random data the maximum frequency of an episode falls rapidly with size of episode and it is less than 10 for size 3 onwards. On the other hand, if we generate data with specific pattern of interconnections then even the minimum frequency of episodes that are part of the mebedded pattern is about two orders of magnitude higher. In all these tables we have used an inter-event time constraint of 0.004–0.006 sec. For random data generated through interconnected neurons model, this is reasonable because we have a synaptic delay of 0.005 sec. However, one may argue that in data generated

Size	Max. Episode Frequency		
	Avg	Max	Min
1-Node	1249.00	1513.00	1004.00
2-Node	78.22	113.00	51.00
3-Node	10.22	15.00	7.00
4-Node	3.54	6.00	3.00
5-Node	2.10	3.00	2.00
6-Node	1.24	2.00	0.00
7-Node	0.10	2.00	0.00
8-Node	0.00	0.00	0.00
9-Node	0.00	0.00	0.00
10-Node	0.00	0.00	0.00
Sample size = 100			

Table 17: Statistics for serial episode mining on random spike sequences generated using random (fized or varying) firing rates for neurons. (Serial Episode Inter-event time constraint = 0.004-0.006 sec) For different sizes of episodes, we show the maximum frequency of any episode of that size. Each entry shows the maximum, minimum and average values of the maximum frequency. These statistics are obtained from a sample size of 100 data sets

Size	Min. Episode Frequency		
	Avg	Max	Min
1-Node	967.80	1032.00	916.00
2-Node	845.65	903.00	798.00
3-Node	734.55	770.00	702.00
4-Node	647.30	679.00	608.00
5-Node	576.06	615.00	548.00
6-Node	515.88	545.00	482.00
7-Node	466.33	487.00	448.00
8-Node	423.58	447.00	405.00
9-Node	385.25	395.00	376.00
10-Node	353.88	368.00	345.00
Sample size = 20			

Table 18: Statistics for parallel episode mining on spike sequence data with embedded patterns in it. (Serial Episode Inter-event time constraint = 0.004-0.006 sec) For different sizes of episodes, we show the minimum frequency of any episode of that size which is a subepisode of the embedded pattern. Each entry shows the maximum, minimum and average values of the minimum frequency. These statistics are obtained from a sample size of 20 data sets

Size	Max. Episode Frequency		
	Avg	Max	Min
1-Node	1249.00	1513.00	1004.00
2-Node	81.48	115.00	56.00
3-Node	11.62	20.00	8.00
4-Node	4.41	6.00	3.00
5-Node	2.87	4.00	2.00
6-Node	2.05	3.00	2.00
7-Node	2.00	2.00	2.00
8-Node	1.46	2.00	0.00
9-Node	0.44	2.00	0.00
10-Node	0.10	2.00	0.00
Sample size = 100			

Table 19: Statistics for serial episode mining with inter-event time constraint discovery on data sets generated with (fixed or varying) random firing rates. The set of possible inter-event time constraints are: 0.002-0.004 sec, 0.004-0.006 sec, 0.006-0.008 sec. As before we show statistics of maximum observed frequencies for episodes of different sizes

through random firing rates, there may be episodes with higher frequencies if we consider other inter-event time constraints. So, on these sets of random data, we have used our mining algorithm that can automatically detect the best possible inter-event constraint from a given set of constraints. These results are shown in Table 19. It is easily seen that even in this case, the frequencies of episodes fall off very rapidly with episode size. Fig. 11 shows the plot of episode frequencies versus size in case of serial episodes in noise data as well as in data with patterns embedded in it.

All the above results clearly demonstrate that it is extremely unlikely to have large size episodes with any appreciable frequencies in random spike data. For example, from the above results we can conclude that the probability of having an episode of size greater than 2 with a frequency of 300 under the null hypothesis is less than 0.005 because not even once in 200 samples from the Null hypothesis did we get an episode of this frequency. This then is the p-value for asserting that an episode of frequency above 300 is significant. Of course, given the vast difference between frequencies of episodes in random and patterned data, such p-values are really not important. From the tables, it is also clear that frequency threshold of 250 or 300 (in data of this length) brings out only significant patterns.

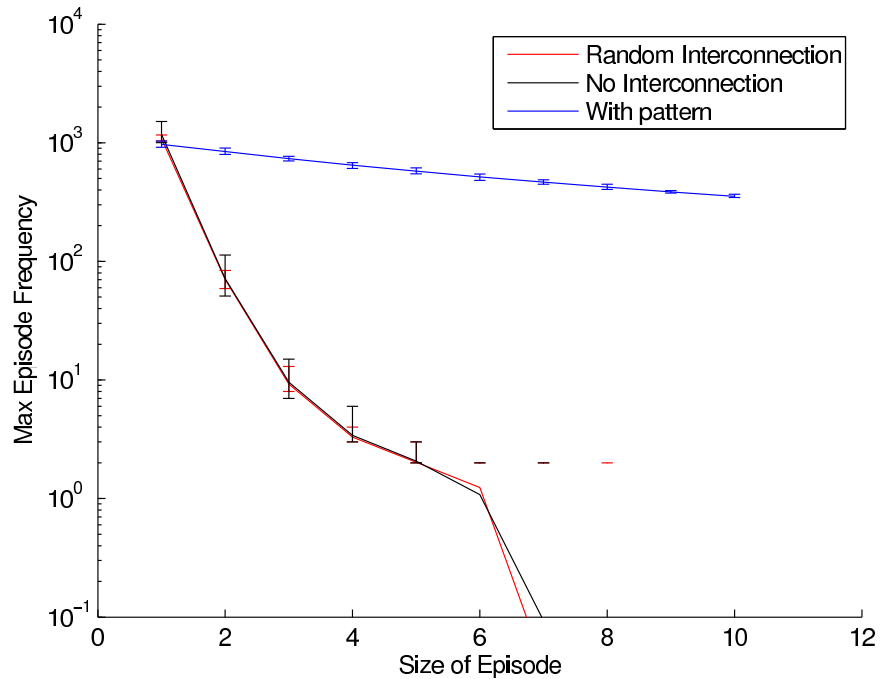


Figure 11: Differences in episode frequencies in noise sequences and sequences with patterns. All are serial episodes with inter-event time constraint of 0.004–0.006 sec. For the case of data with patterns, we show minimum frequency for any episode that is part of the embedded pattern and the error bars show the range of variation. The figure clearly shows that it is extremely unlikely to have episodes of size 3 or more with appreciable frequency ‘by chance’.

Given a specific data set (which may be obtained through experiments on neural cultures) one can use the above method for assessing significance of discovered episodes as follows. From the data we estimate average firing rates of individual neurons and also firing rates averaged over windows of appropriate width. We use these to set the random firing rates as well as the variations in firing rates in our models for generating the random data sets. Then we generate many random data sets of the same length as the given data and discover episodes with the same temporal constraints as in the real data. Then, by comparing frequencies as above, we can say which of the discovered episodes are significant. As a matter of fact, using the distribution of frequencies in the random data, we can set the frequency thresholds for our algorithms to discover significant episodes in the real data.

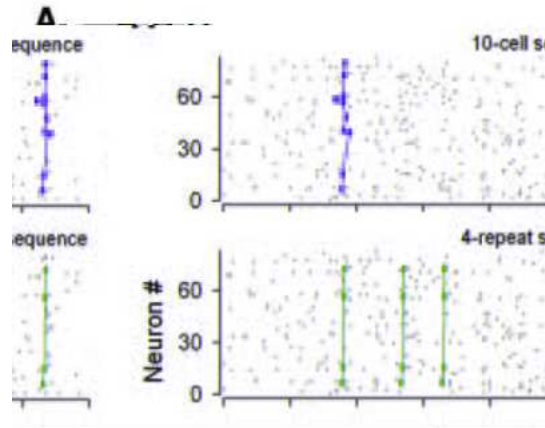


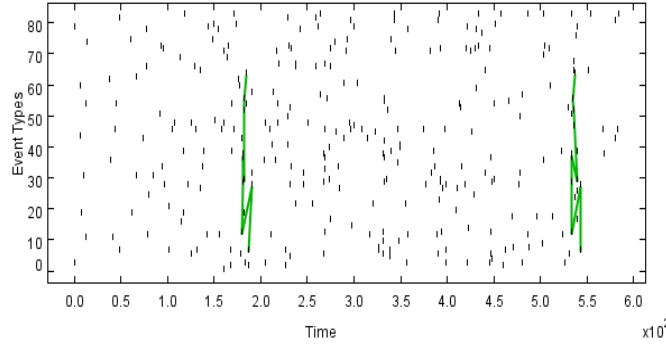
Figure 12: Repeated motifs during sequential reactivation of identical cells (A) Set of neurons with precise sequences of calcium transients (V1 slice). Ten cells reactivated with exact timings between their transients (top panel). In the same raster plot, a four-cell sequence is reactivated four times (middle panel). This four-cell sequence also acted as a part of the 10-cell sequence. Bottom panel shows all sequences detected in the same raster plot.

5.4 Analysis of multi-neuron data obtained through Calcium Imaging

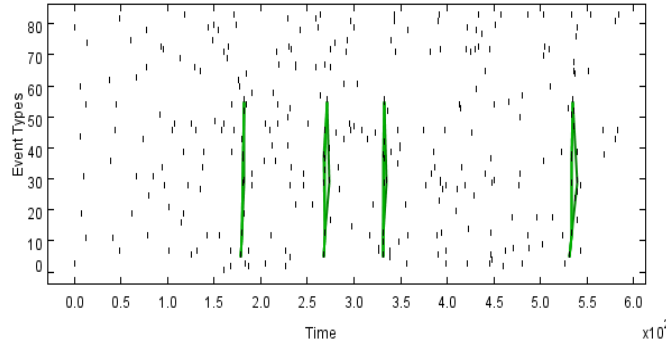
In this section we describe results obtained on data sets collected from experiments on neural ensembles. This data set is from Dr. Rafael Yuste's² lab in Dept. of Biological Sciences, Columbia University, New York and the results of these experiments are reported in [1]. In this experiment, the data is obtained through calcium imaging technique. In [1], Ikegaya et. al. analyzed how neural activity propagates through cortical networks. They found precise repetitions of spontaneous patterns. These patterns repeated after minutes maintaining millisecond accuracy. In Fig. 3A of [1], such patterns are shown in raster plots by connecting the spikes that are part of an occurrence.

Fig. 12 shows a figure reproduced from [1] along with its original caption. In Fig. 13, we show results obtained on the same calcium imaging data set using frequent episode discovery algorithms. Fig. 13 (a) shows two occurrences of a 10-node parallel episode discovered with expiry time constraint $T_X = 10$ time

²We are extremely grateful to Dr. Rafael Yuste for sharing the calcium imaging data with us.



(a) Frequent parallel episodes of size 10 satisfying expiry constraint = 10 time units



(b) Frequent serial episodes of size 4 satisfying inter-event interval constraint = 10 time units

Figure 13: Frequent episodes discovered using our algorithms on real data.

units. Fig. 13 (b) shows four occurrences of a 4-node serial episode discovered with inter-event constraint of 0 to 10 time units. It is seen that the results obtained using frequent episode discovery match with those presented in [1] by comparing figures 12 with 13. Also, the time needed by our algorithm is much smaller because in [1], they use a counting technique that can not control the combinatorial explosion. This result brings out the utility of our data mining technique in terms of both effectiveness and efficiency.

5.5 Analysis of multi-neuron data obtained through multi-electrode array experiments

In this subsection we present some of the results we obtained with our algorithms on multi-neuronal data obtained through multi-electrode array experiments.³ The data is obtained from dissociated cultures of cortical neurons grown on multi-electrode arrays. This is an extremely rich set of data where 58 cultures of varying densities are followed for five weeks. Everyday, the spontaneous activity as well as stimulated activity of each culture is recorded for different time durations. (See [2] for the details of experiments, nature of data, trends observed etc.). Since data was recorded from each culture for many days, one can presumably infer development of connections also. Here we only present a few of the results we obtained from analyzing the spontaneous data from these cultures, to illustrate the utility of our temporal datamining techniques.

In these dissociated cortical cultures, there is a lot of spontaneous activity including many cycles of network-wide bursts [2]. Thus, patterns of coordinated firing by groups of neurons, even when they exist, would be rare in the sense that the spikes which form the coordinated activity constitute only a small fraction of the total number of spikes output by the system. Thus, simple cross correlation based methods are not very effective in unearthing coordinated firing patterns. Using our algorithm for serial episode discovery under inter-event constraints, we are able to obtain some frequent episodes which remain frequent for a large number of days with increasing trend in frequency.

Fig. 14 shows a few such serial episodes discovered in the data from one of the cultures. (We have used inter-event time constraint of 0–5 milli sec). The figure plots the frequency (in terms of the number of non-overlapping occurrences as a fraction of the data length) for the frequent serial episodes versus the day on which the data is collected. In the figure, c5, e5, e6, d6 etc. are the pin numbers in the multi-electrode array which will be event types for the data mining algorithms. The increasing trend of the frequency is very clear and it is highly plausible that these episodes represent some underlying microcircuits that are developing as the culture ages. Fig. 15 shows some further analysis of one of the episodes discovered, namely, $f8 \rightarrow g8 \rightarrow d8$. The figure plots ratio

³We are grateful to Prof. Steve Potter, Georgia Institute of Technology and Emory University, Atlanta, USA, for providing the data and for many useful discussions on analyzing this data.

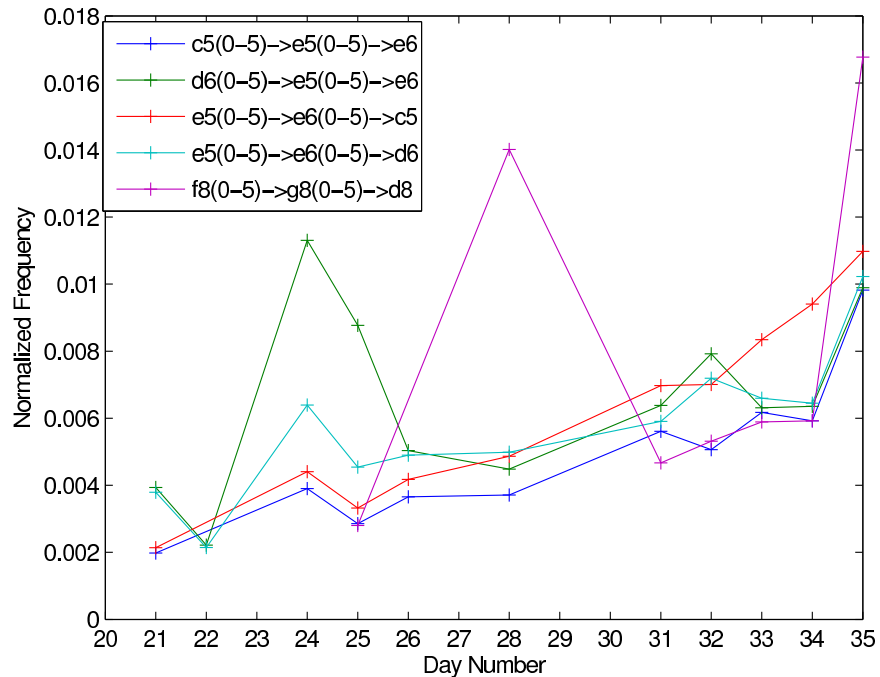


Figure 14: Some frequent Serial Episodes discovered from multi-electrode array data from [2]. We plot the normalized frequency versus the age in days of the culture. These are from data of culture 2-1.

of the frequencies of $f8 \rightarrow g8$ to that of $f8$ and similarly for $g8 \rightarrow d8$ and $g8$. This ratio, which we call the confidence for the subepisode, gives an indication of the chance that the second neuron spikes given the first one spiked. If the episode is really due to a circuit, we expect this confidence to be high but not too high. (If a spike from electrode $g8$ always follows a spike from electrode $f8$, then it may be that a single axon is making contact with both electrodes). As can be seen from the figure, the confidence values steadily grow with age of the culture and reach a reasonably high value. The increasing trend of the confidence values matches well with the increasing trend of the frequency of the episode also thus indicating that some underlying structure is responsible for the repeated occurrence of this episode. Similar behaviour is seen in case of other episodes and also for other cultures, thus indicating that the frequent episodes discovered are most probably due to coordinated firing by some group of neurons due to some underlying structures in the culture.

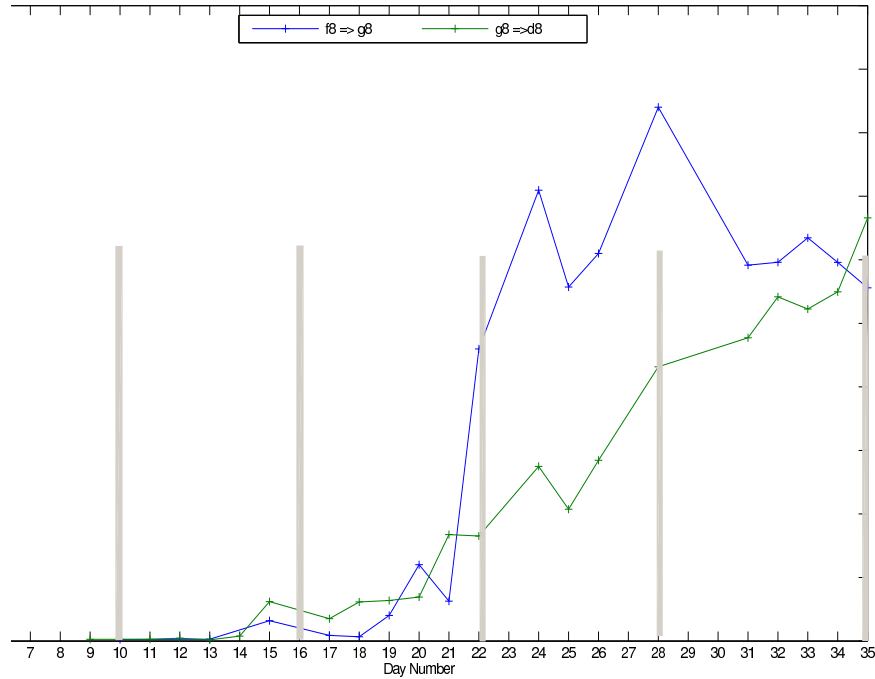


Figure 15: Confidence scores for subepisodes of the episode $f8 \rightarrow g8 \rightarrow d8$ versus age of culture in days. See text for explanation

In this data, there is no ground truth available regarding connections and hence it is not possible to directly validate the discovered episodes. However, we can indirectly get some evidence that the episodes capture some underlying structure in the neural system by looking at the sets of episodes obtained from same culture on different days and from different cultures. We considered six cultures, namely, culture 2-1 to culture 2-6. For each culture we considered the data from the last five days, namely days 31 to 35. (As we have seen from earlier figures, the circuits seem to stabilize only in the last week). However, in our data set, for culture 2-4 there was no recording on day 34 Thus we have 29 data sets such as 2-1-31 (meaning culture 2-1, day 31) and so on. From each culture on each day, we have 30 minutes of data recording spontaneous activity. From each data set, we have taken a 10 minute duration data slice. From each such data slice, we identified top twenty most frequent 7-node serial episodes with inter-event interval constraint of 0–5 milli sec. (We want to consider long episodes because, as we saw earlier, it is highly unlikely to have large

size frequent episodes by chance. The size of 7 is chosen so that all data sets have atleast twenty episodes of that size). Now we want to compare the sets of episodes discovered from different data slices. For this we need a measure of similarity between sets of episodes.

We define a similarity score for two sets, A, B , of episodes of size, say, N , as follows. We first count the number of N -node episodes that are common in the two sets and remove all the common ones from both sets. Then we replace each episode (in each set) with the two $(N-1)$ -node subepisodes obtained by dropping the first or last nodes in the original episode. We now count the common $(N-1)$ -node episodes (in the two sets) and remove them. We go on like this, by replacing the left-over episodes with subepisodes of size one less and counting the common ones, till we reach episodes of size 1. Let n_i denote the number of common episodes of size i . Then the similarity between the sets A and B is defined as

$$\text{Sim}(A, B) = \sum_{i=1}^N 2^i n_i.$$

Since we want to view episodes as representing connections, similarity has to capture how much of the paths represented by different episodes are common. The above measure does just that and gives higher weightage to common long episodes.

Fig. 16 shows the cross-similarity between the sets of frequent episodes from the 29 data slices by colour coding similarity values. The axes indicate the culture-day combinations. Note that the two axes are ordered differently so that the reverse diagonal represents similarity between identical sets of episodes. That is why the reverse diagonal has highest similarity values. What is interesting is that data slices from the same culture but from different days are highly similar. This can be seen by observing the 5×5 submatrices around the reverse diagonal in the figure. (For the 2-4 culture, this submatrix is only 4×4 because there is no data for 2-4-34). This is in sharp contrast to the fact (as seen from the figure) that sets of episodes obtained from different cultures have very low similarity. These results strongly support the view that the frequent episodes capture some underlying structure in the neural system.

As said earlier, in the data we are considering, all cultures show very strong network-wide bursting activity that keeps occurring again and again. It is observed that most of our long episodes occur only during the burst period. Hence,

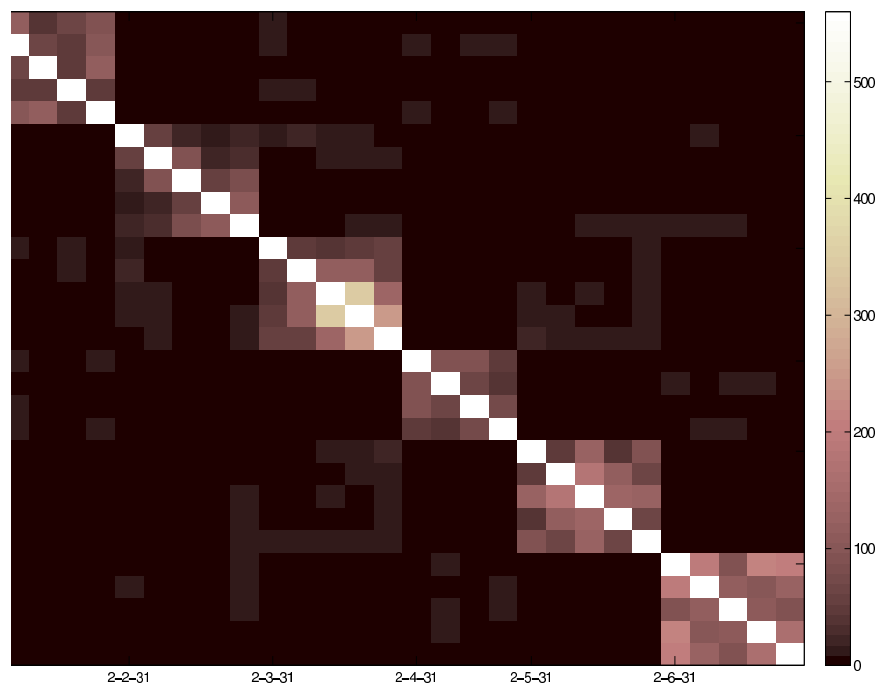


Figure 16: Cross similarity between sets of frequent Serial Episodes. Each point represents similarity score between two sets of frequent episodes obtained from 10 minute duration data from pairs of culture-day combinations. Since the two axes are ordered in reverse orders, the reverse diagonal corresponds to the case where the two sets of frequent episodes are identical. The colour code is explained by the legend on the right. Note the high similarity scores around the reverse diagonal showing that sets of episodes from the same culture are much more similar than those from different cultures.

an interesting question to ask is how far are individual bursts characterize the underlying system. For this, we do a similar analysis as above. As earlier, we obtain 29 sets of frequent episodes by taking ten minute data from each culture on each of days 31 to 35. We then get another 29 sets of frequent episode from data corresponding to a single burst (taken outside the ten minute duration) from each culture on each of the days 31 to 35. We then obtain similarities between these sets of frequent episodes and the results are shown in fig. 17. As can be seen, the results are strikingly similar to the earlier case. Frequent episodes obtained from different cultures are highly dissimilar while those from the same culture but from different days are much more similar. The main difference here as compared to the earlier case, is along the reverse diagonal in the figure,

where, while the similarity values are high, they are not the highest as in the earlier case. This is because (for the points along the reverse diagonal), one set of frequent episodes is obtained from data of ten minute duration whereas the other set is obtained from only a single burst which is typically only a couple of seconds long. In spite of this, these two sets of episodes show good similarity if they are from the same culture. This once again supports the view that there are some characteristic structures that are different for different cultures (which is natural because the synapses that form in a culture are mostly random) and these are captured well by our frequent episodes.

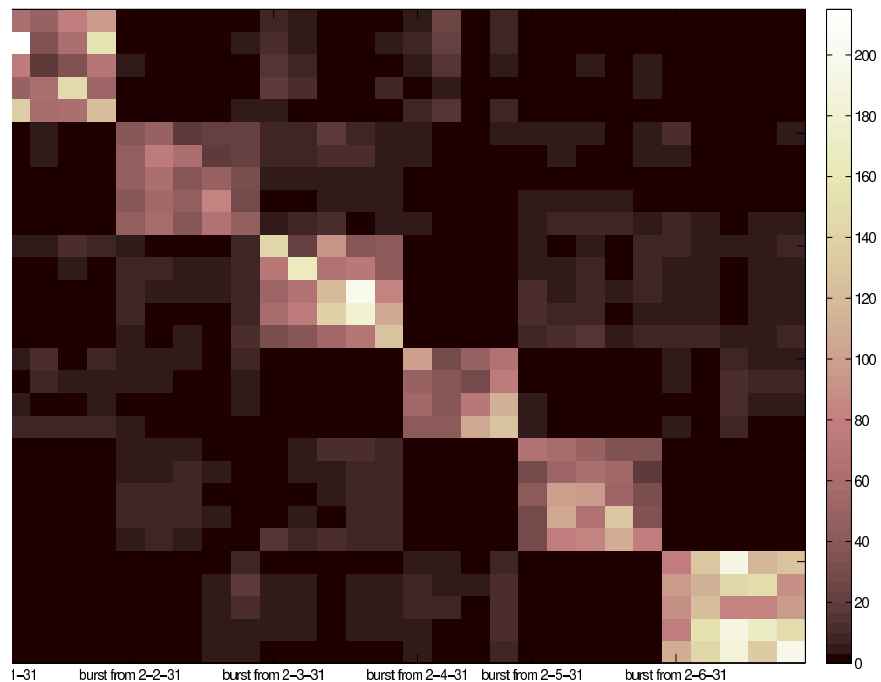


Figure 17: Similarity between sets of frequent Serial Episodes. Each point represents similarity score between two sets of frequent episodes, one obtained from a 10 minute duration data and the other from a single burst, corresponding to pairs of culture-day combinations. Since the two axes are ordered in reverse orders, the reverse diagonal corresponds to same culture-day combinations. The colour code is explained by the legend on the right. Note the high similarity scores around the reverse diagonal showing that sets of episodes from the same culture are much more similar than those from different cultures.

The results presented in figures 16 and 17 strongly indicate that the set of frequent episodes seem to characterize the activity of a neural culture well and

hence they capture the underlying microcircuits which are different for different cultures.

6 DISCUSSION

In this paper we have considered the problem of analyzing multi-neuronal spike data sequences. We argued that the temporal data mining framework of frequent episode discovery is a very useful formalism for addressing this problem. We have shown how the structure of episodes with additional temporal constraints can capture most of the patterns that are of interest in this area of neurobiology. We have presented algorithms for discovering such frequent episodes and illustrated the performance of the algorithms through simulations. We have considered both synthetic data generated through a realistic neuronal spike simulator as well as two sets of multi-neuronal data – one obtained through Calcium imaging and the other obtained from multi-electrode array experiments. We have also presented extensive empirical results to show that our frequent episodes represent statistically significant patterns of correlated firings in the underlying neural system.

Analyzing multi-neuron spike data is a challenging problem of much current interest in neuroscience. Due to the abundance of experimental techniques one can now obtain data representing the simultaneous activity of many neurons grown *in vivo*. Thus algorithms that can unearth significant patterns in the data would go a long way in allowing neurobiologists to study firing patterns and microcircuits in neural assemblies. Such an understanding of the behaviour of interacting neurons is very useful in understanding vital issues such as learning and memory as well as for concrete applications such as brain computer interfaces.

We have shown how one can detect many coordinated firing patterns such as order, synchrony as well as synfire chains in terms of episodes with appropriate temporal constraints. We illustrated the effectiveness of the algorithms by analyzing synthetically generated spike sequences that have embedded patterns in them. For this we have modelled each neuron as an inhomogeneous Poisson process whose spiking rate gets modified in response to the input received from other neurons. By building an interconnected system of such neurons with some specific large excitatory connections along with many random connections

we can embed different patterns in the system that is generating the spike data. Since the ground truth is known in these sequences, they serve as a useful test bed for assessing the capabilities of our algorithms. We have shown that our algorithms unerringly discover the underlying structure and also that they scale well even if there are multiple such patterns in the data.

We have also used our neuronal spike data simulator to show that the kind of episodes we are taking about do not happen by chance. We have generated many sets of random data of both independent and dependent neurons and by using the ‘jitter method’ [11] idea of sampling from a null hypothesis are able to show that the maximum frequency of episodes in noise data are orders of magnitude smaller than minimum frequencies of relevant episodes when data contains patterns. This, we feel, is a very significant contribution of this paper because the null hypothesis we consider here goes far beyond the usual one of independent homogeneous Poisson processes.

We have also illustrated the effectiveness of our method in analyzing data obtained from multi-neuronal systems grown in vivo. These results also show that, unlike the methods based on correlations, the data mining techniques proposed here are much more promising for getting information regarding the connectivity patterns.

The data mining techniques we proposed here are much more efficient than the current methods based on analyzing correlations between spike trains and are also seen to be much more effective in unearthing interesting patterns that are relevant to understanding connectivity patterns. However, the full data analysis problem is very challenging because the spike trains are noisy stochastic processes where the useful patterns of coordinated activity can often be submerged by vast amount of background spiking. Thus, we view the results of this paper more as indicative of what the data mining approach can offer in this area rather than as solving the problem. Much more work is needed to develop these techniques to a level where they can become a routine tool for neurobiologists. We hope that this paper would contribute towards developing the necessary collaborations between neurobiologists and data mining researchers for such a fruitful activity.

References

- [1] Y. Ikegaya, G. Aaron, R. Cossart, D. Aronov, I. Lampl, D. Ferster, and R. Yuste, “Synfire chains and cortical songs: temporal modules of cortical activity,” *Science*, vol. 304, pp. 559–564, Apr 2004.
- [2] D. A. Wagenaar, J. Pine, and S. M. Potter, “An extremely rich repertoire of bursting patterns during the development of cortical cultures,” *BMC Neuroscience*, 2006.
- [3] H. Mannila, H. Toivonen, and A. Inkeri Verkamo, “Discovery of frequent episodes in event sequences,” *Data Mining and Knowledge Discovery*, vol. 1, pp. 259–289, September 1997. doi:10.1023/A:1009748302351.
- [4] S. Laxman, P.S.Sastry, and K. Unnikrishnan, “Discovering frequent episodes and learning hidden markov models: A formal connection,” *IEEE Transactions on Knowledge and Data Engineering*, vol. 17, no. 11, pp. 1505–1517, 2005.
- [5] D. Patnaik, *Application of frequent episode discovery framework in micro-electrode array data analysis*. ME thesis, Indian Institute of Science, June 2006.
- [6] S. Laxman and P.S.Sastry, “A survey of temporal data mining,” *SAD-HANA, Academy Proceedings in Engineering Sciences*, 2005.
- [7] M. Abeles and G. L. Gerstein, “Detecting spatiotemporal firing patterns among simultaneously recorded single neurons,” *J Neurophysiol*, vol. 60, pp. 909–924, Sep 1988.
- [8] A. K. Lee and M. A. Wilson, “A combinatorial method for analyzing sequential firing patterns involving an arbitrary number of neurons based on relative time order,” *J Neurophysiol*, vol. 92, no. 4, pp. 2555–2573, 2004.
- [9] I. V. Tetko and A. E. Villa, “A pattern grouping algorithm for analysis of spatiotemporal patterns in neuronal spike trains. 1. detection of repeated patterns,” *J Neurosci Methods*, vol. 105, pp. 1–14, Jan 2001.
- [10] R. Agrawal and R. Srikant, “Fast algorithms for mining association rules,” in *Proc. 20th Int. Conf. Very Large Data Bases, VLDB* (J. B. Bocca,

- M. Jarke, and C. Zaniolo, eds.), pp. 487–499, Morgan Kaufmann, 12–15 1994.
- [11] A. Date, E. Bienenstock, and S. Geman, “On the temporal resolution of neural activity,” 1998.
- [12] M. Meister, J. Pine, and D. A. Baylor, “Multi-neuronal signals from the retina: acquisition and analysis,” *J Neurosci Methods*, vol. 51, pp. 95–106, Jan 1994.
- [13] M. Meister, “Multineuronal codes in retinal signaling,” *Proc Natl Acad Sci U S A*, vol. 93, pp. 609–614, Jan 1996.
- [14] M. A. L. Nicolelis, D. Dimitrov, J. M. Carmena, R. Crist, G. Lehew, J. D. Kralik, and S. P. Wise, “Chronic, multisite, multielectrode recordings in macaque monkeys,” *PNAS*, vol. 100, no. 19, pp. 11041–11046, 2003.
- [15] G. L. Gerstein, “Searching for significance in spatio-temporal firing patterns,” *Acta Neurobiol Exp (Wars)*, vol. 64, no. 2, pp. 203–207, 2004.
- [16] K. D. Wise, D. J. Anderson, J. F. Hetke, D. R. Kipke, and K. Najafi, “Wireless implantable microsystems: high-density electronic interfaces to the nervous system,” *Proceedings of the IEEE*, vol. 92, pp. 76–97, Jan 2004.
- [17] T. Hosoya, S. A. Baccus, and M. Meister, “Dynamic predictive coding by the retina,” *Nature*, vol. 436, pp. 71–77, July 2005. 10.1038/nature03689.
- [18] D. H. Perkel, G. L. Gerstein, and G. P. Moore, “Neuronal spike trains and stochastic point processes ii: simultaneous spike trains,” *Biophysical Journal*, vol. 7, pp. 419–440, 1967.
- [19] E. N. Brown, R. E. Kass, and P. P. Mitra, “Multiple neural spike train data analysis: state-of-the-art and future challenges,” *Nat Neurosci*, vol. 7, pp. 456–461, May 2004. 10.1038/nm1228.
- [20] T. Hosoya, S. A. Baccus, and M. Meister, “Dynamic predictive coding by the retina,” *Nature*, vol. 436, pp. 71–77, Jul 2005.
- [21] A. Riehle, S. Grun, M. Diesmann, and A. Aertsen, “Spike Synchronization and Rate Modulation Differentially Involved in Motor Cortical Function,” *Science*, vol. 278, no. 5345, pp. 1950–1953, 1997.

- [22] A. Riehle, F. Grammont, M. Diesmann, and S. Grun, “Dynamical changes and temporal precision of synchronized spiking activity in monkey motor cortex during movement preparation,” *Journal of Physiology-Paris*, vol. 94, no. 569-582, 2000.
- [23] M. J. Schnitzer and M. Meister, “Multineuronal firing patterns in the signal from eye to brain,” *Neuron*, vol. 37, pp. 499–511, Feb 2003.
- [24] M. Abeles and I. Gat, “Detecting precise firing sequences in experimental data,” *J Neurosci Methods*, vol. 107, pp. 141–154, May 2001.
- [25] A. K. Lee and M. A. Wilson, “Memory of sequential experience in the hippocampus during slow wave sleep,” *Neuron*, vol. 36, pp. 1183–1194, Dec 2002.
- [26] S. Laxman, *Discovering Frequent Episodes: Fast algorithms, connection with HMMs and generalization*. PhD thesis, Indian Institute of Science, March 2006.
- [27] R. Agrawal and R. Srikant, “Mining sequential patterns,” in *Eleventh International Conference on Data Engineering* (P. S. Yu and A. S. P. Chen, eds.), (Taipei, Taiwan), pp. 3–14, IEEE Computer Society Press, 1995.
- [28] A. Amarasingham, *Statistical methods for the assessment of temporal structure in the activity of the nervous system*. PhD thesis, Division of Applied Mathematics, Brown University, Providence, RI, USA, 2004.

A Pseudo-code listing for Algorithms in the paper

Algorithm 2 Non-overlapped count for parallel episodes with expiry time constraint

Input: Set C of candidate N -node parallel episodes, event streams $s = \langle (E_1, t_1), \dots, (E_n, t_n) \rangle$, frequency threshold $\lambda_{min} \in [0, 1]$, expiry time T_x

Output: The set F of frequent serial episodes in C

```

1: for all event types  $A$  do
2:    $waits(A) = \phi$ 
3: for all  $\alpha \in C$  do
4:   Initialize  $autos(\alpha) = \phi$ 
5: for all  $\alpha \in C$  do
6:   for all event types  $A \in \alpha$  do
7:     Create node  $s$  with  $s.episode = \alpha$ ;  $s.init = 0$  ;
8:      $s.count = 1$ 
9:     Add  $s$  to  $waits(A)$ 
10:    Add  $s$  to  $autos(\alpha)$ 
11:   Set  $\alpha.freq = 0$ 
12:   Set  $\alpha.counter = 0$ 
13: for  $i = 1$  to  $n$  do
14:   for all  $s \in waits(E_i)$  do
15:     Set  $\alpha = s.episode$ 
16:     Set  $j = s.count$ 
17:     if  $j > 0$  then
18:       Set  $s.count = j - 1$ 
19:        $\alpha.counter = \alpha.counter + 1$ 
20:      $s.init = t_i$ 
21:     {Expiry check}
22:     if  $\alpha.counter = N$  then
23:       for all  $q \in autos(\alpha)$  do
24:         if  $(t_i - q.init) > T_x$  then
25:            $\alpha.counter = \alpha.counter - 1$ 
26:            $q.count = q.count + 1$ 
27:       {Update episode count}
28:     if  $\alpha.counter = N$  then
29:       Update  $\alpha.freq = \alpha.freq + 1$ 
30:       Reset  $\alpha.counter = 0$ 
31:       for all  $q \in autos(\alpha)$  do
32:         Update  $q.count = 1$ 
33: Output  $F = \{\alpha \in C \text{ such that } \alpha.freq \geq n\lambda_{min}\}$ 

```

Algorithm 3 Non-overlapped serial episodes count with inter-event interval constraints

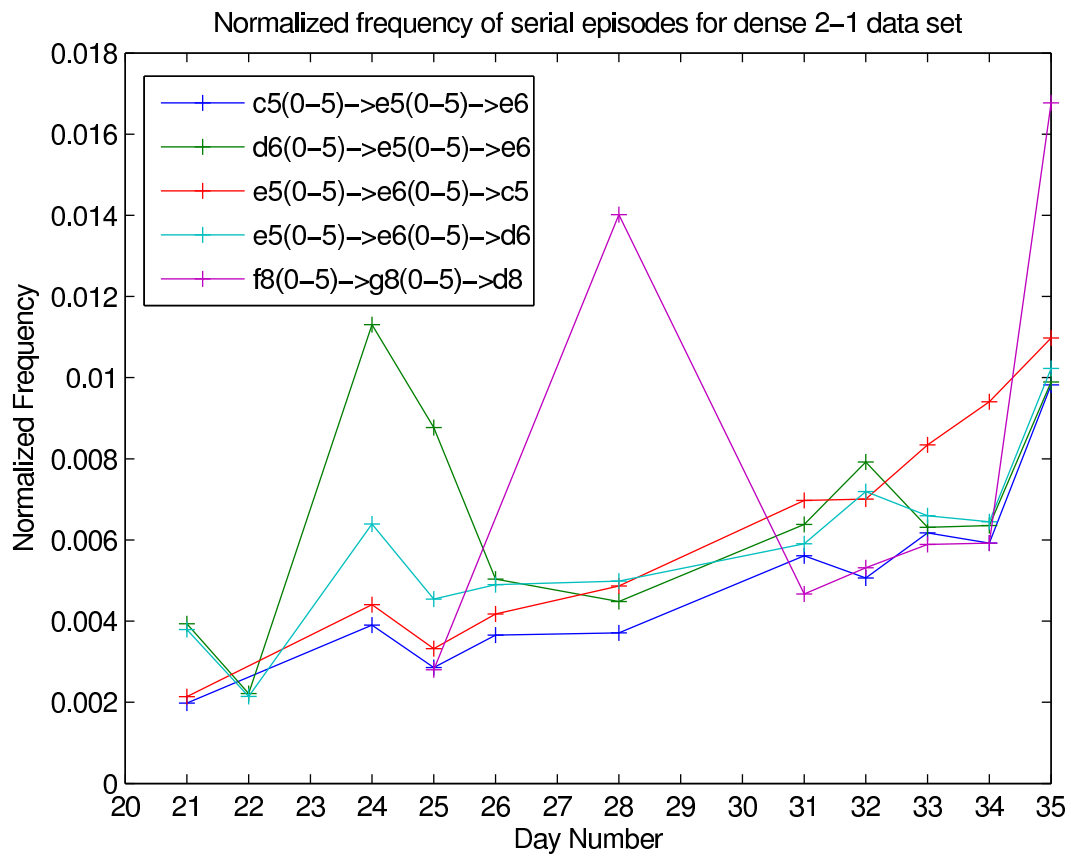
Input: Set C of candidate N -node parallel episodes, event streams $s = \langle (E_1, t_1), \dots, (E_n, t_n) \rangle$, frequency threshold $\lambda_{min} \in [0, 1]$, expiry time T_X

Output: The set F of frequent serial episodes in C

```

1: for all event types  $A$  do
2:   Initialize  $waits(A) = \phi$ 
3: for all  $\alpha \in C$  do
4:   Set  $prev = \phi$ 
5:   for  $i = 1$  to  $N$  do
6:     Create  $node$  with  $node.visited = false$ ;  $node.episode = \alpha$ ;
        $node.index = i$ ;  $node.prev = prev$ ;  $node.next = \phi$ 
7:     if  $i = 1$  then
8:       Add  $node$  to  $waits(\alpha[1])$ 
9:     if  $prev \neq \phi$  then
10:       $prev.next = node$ 
11:    for  $i = 1$  to  $n$  do
12:      for all  $node \in waits(E_i)$  do
13:        Set  $accepted = false$ 
14:        Set  $\alpha = node.episode$ 
15:        Set  $j = node.index$ 
16:        Set  $tlist = node.tlist$ 
17:        if  $j < N$  then
18:          for all  $tval \in tlist$  do
19:            if  $(t_i - tval.init) > \alpha.t_{high}[j]$  then
20:              Remove  $tval$  from  $tlist$ 
21:          if  $j = 1$  then
22:            Update  $accepted = true$ 
23:            Update  $tval.init = t_i$ 
24:            Add  $tval$  to  $tlist$ 
25:            if  $node.visited = false$  then
26:              Update  $node.visited = true$ 
27:              Add  $node.next$  to  $waits(\alpha[j + 1])$ 
28:          else
29:            for all  $prev\_tval \in node.prev.tlist$  do
30:              if  $t_i - prev\_tval \in (\alpha.t_{low}[j - 1], \alpha.t_{high}[j - 1])$  then
31:                Update  $accepted = true$ 
32:                Update  $tval.init = t_i$ 
33:                Add  $tval$  to  $tlist$ 
34:                if  $node.visited = false$  then
35:                  Update  $node.visited = true$ 
36:                  if  $node.index \leq N - 1$  then
37:                    Add  $node.next$  to  $waits(\alpha[j + 1])$ 
38:                else
39:                  if  $t_i - prev\_tval > \alpha.t_{high}[j - 1]$  then
40:                    Remove  $prev\_tval$  from  $node.prev.tlist$ 
41:            if  $accepted = true$  and  $node.index = N$  then
42:              Update  $\alpha.freq = \alpha.freq + 1$ 
43:              Set  $temp = node$ 
44:              while  $temp \neq \phi$  do
45:                Update  $temp.visited = false$ 
46:                if  $temp.index \neq 1$  then
47:                  Remove  $temp$  from  $waits(\alpha[temp.index])$ 
48:                Update  $temp = temp.next$ 
49: Output  $F = \{\alpha \in C \text{ such that } \alpha.freq \geq n\lambda_{min}\}$ 

```



Confidence of A=>B for 2-1 data set

